# AN INDEX FOR ANTICIPATING EXCESSIVE PRECIPITATION WITH ELEVATED THUNDERSTORMS

---

A Thesis

presented to

the Faculty of the Graduate School

at the University of Missouri-Columbia

---

In Partial Fulfillment

of the Requirements for the Degree

Master of Science

---

by

ALZINA FOSCATO

Dr. Patrick Market, Thesis Advisor

JULY 2016

The undersigned, appointed by the dean of the Graduate School, have examined the thesis entitled

AN INDEX FOR ANTICIPATING EXCESSIVE PRECIPITATION WITH ELEVATED THUNDERSTORMS

Presented by Alzina Foscato,

a candidate for the degree of master of science,

and hereby certify that, in their opinion, it is worthy of acceptance.

Professor Patrick Market

Professor Neil Fox

Professor Charles Nilon

# Acknowledgements

I would first like to thank Dr. Patrick Market for allowing me to be one of his graduate students and for finding an epic research project with funding my second year of graduate work. I'm also very thankful to the National Science Foundation for funding this research as well as my second year in graduate school. I would like to thank Dr. Neil Fox and Dr. Charles Nilon for being on my thesis committee. I'd like to thank Dr. Market, Dr. Fox, Dr. Anthony Lupo, and Dr. Bohumil Svoma for teaching me everything I know about Atmospheric Science, and for being really easy to go to when I have questions or problems. I would also like to thank the other graduate students for helping encourage me and help guide me through any problems that I had with course or my research. I would also like to thank Jaret Rogers, Steven Weiss, Isreal Jirak and Chris Melick for helping with gathering data for this project.

Finally, I would like to thank my daughter Gracie Lynn for her loving support and understanding of what I had to accomplish to get where I am today. She was always patient when I had to study or write and couldn't find time to go outside. I am very blessed to have such a wonderful child who knew that I could do anything. I am also very blessed to have such supportive friends here in Missouri to be there for me when my distant family couldn't. I am also thankful for my family understanding that I need to stay here in Missouri to get the degree that I always dreamed of.

# Contents

# Figures

# Tables

# Chapter 1. Introduction

Attempting to predict the location and the initiation of elevated thunderstorms can be very challenging due to the uncertainty in of the mechanisms that release elevated instability (Moore et al., 2003). Excessive Precipitation with Elevated Convection (EPEC) is a parameter that was created in order to help predict where heavy rainfall associated with elevated convection will occur.

## 1.1 Purpose

The two most common severe threats that are associated with elevated thunderstorms are heavy rainfall, which can lead to flash flooding, and hail (Grant, 1995). Flash flooding is common during all seasons but is most common in the summer months (Maddox et al., 1979). Forecasting for thunderstorms that develop north of a surface front can be problematic due to the cool and stable conditions at the surface (Grant, 1995).

The purpose for this research is to verify if EPEC can be used as a predictive parameter for heavy rainfall associated with elevated convection. During 2014 to 2015 the Program of Research on Elevated Convection with Intense Precipitation (PRECIP) project collected data for numerous heavy rainfall events in the Midwestern United States forecasting heavy rainfall events. This study was based upon past events collected during the PRECIP project. EPEC was critical for identifying where heavy rainfall might occur during 2014 and 2015.

## 1.2 Objectives

Forecasting and warning for flash flooding presents a challenge especially when it can lead to damage, injury, and death. This study mainly focuses on verifying if EPEC can be effectively used as a predictive tool for forecasting flash flooding. To achieve the purpose previously mentioned, the following objectives are identified:

- Create verification statistics on the EPEC metric
- Analyze selected forecasts issued by PRECIP group, which included EPEC as a tool
- Present best and worst cases for the EPEC parameter, and determine why they did (not) work well.

# Chapter 2. Background Research

In order to complete the objectives of this research, an extensive literature review has been performed with the goal of understanding the various components of heavy rainfall and flash flooding.

## 2.1 Climatology of Elevated Convection

Colman (1990) defined elevated thunderstorms as those that are isolated from surface diabatic effects and occur above frontal surfaces. Colman (1990) characterized cold sector thunderstorms as elevated and determined that they can still produce severe weather. He recorded over 1000 reports of elevated thunderstorms for 4 years during the months of April to September of 1978 to 1982. During his study he found a bimodal distribution of elevated thunderstorms with a primary maximum in April and a secondary maximum in September. Colman's (1990) results showed that elevated thunderstorms occurred more in the Midwest region of the United States, with a maximum frequency in eastern Kansas (Figure 2.1). He suggested that this distribution is due to the annual distribution for convective instability and midlatitude cyclones over the conterminous United States.

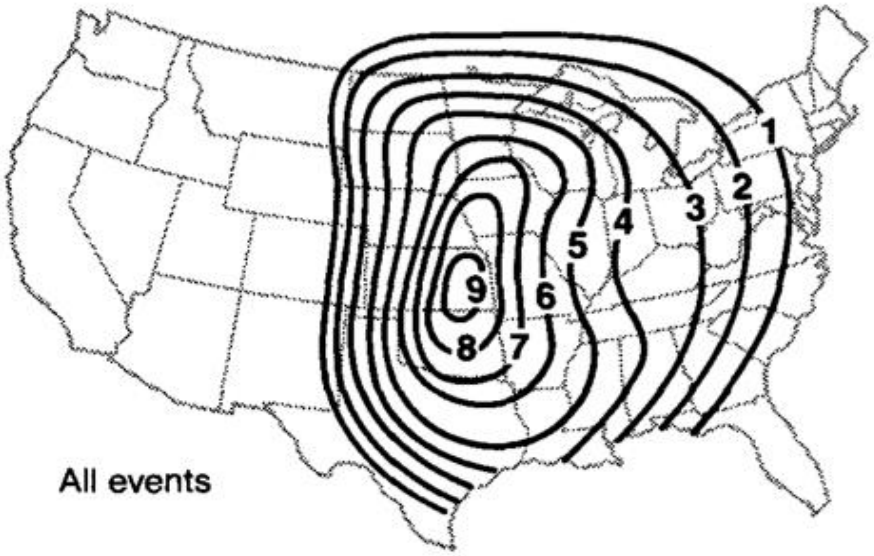


**Figure 2.1. The number of elevated thunderstorms identified over a 4-year period from September through August 1982 (Image and caption reproduced from Colman (1990).**

Colman's (1990) research also showed a diurnal variation of elevated thunderstorms that was influenced by the travel time of the source air over the frontal surface. He found that elevated thunderstorms associated with warm and stationary fronts occur more frequently at 1200 UTC and those with cold fronts more frequent at 0000 UTC. These times were due to the limitation of using soundings at 0000 UTC and 1200 UTC. Colman's (1990) climatology helped define common characteristics that are associated with elevated thunderstorms. These characteristics identified regions and time periods over which elevated thunderstorms could occur.

## 2.2 Heavy Rainfall Associated with Elevated Thunderstorms

During a period of 2 years between 1993 and 1995, Moore et al (1996) collected data on various heavy rainfall events in the Midwestern United States to provide more information on forecasting flash flood events. Many of the cases were the result of elevated thunderstorms, which were on the cold side of a west-east oriented surface boundary. Moore et al (1996) found that the majority of mesoscale convective systems (MCSs) contained elevated thunderstorms, which were a source of heavy rainfall in the central Midwest. The findings of where elevated thunderstorms formed were similar to Colman (1990) except that their seven cases formed in regions of elevated convective instability, which was not commonly found in Colman's study.

The Moore et al. (1996) composite results found that elevated thunderstorms associated with heavy rainfall events were influenced by low-level wind and moisture fields. They also found that the MCSs were about 200 km downstream of the low-level jet maxima and in the right entrance region of the 200 hPa upper-level jet. Moore et al. (1996) also found MCSs were in a region depicted by a stable Lifted Index, slightly unstable Showalter Index and having a relatively high value of the K-index and elevated convective instability between 500 and 850 hPa.

Rochette and Moore(1996) studied an MCS that developed in the morning hours on 06 June 1993 across northern and central Missouri, which produced over 150 mm (6 in.) of heavy rainfall. This MCS occurred in a cool, stable boundary layer just to the north of a surface warm front, which suggests that this storm was elevated. This event was one

of many that aided in the flooding in the Midwestern United States during the summer of 1993. Rochette and Moore (1996) found that the event that occurred on 06 June 1993 showed similarities with Maddox et al.'s (1979) research on frontal flash floods, such as the low-level jet (LLJ) upstream of the MCS initiation point. Even though there were similarities with Maddox et al. (1979), one of the main differences was this event peaked during the late morning hours instead of the common overnight hours.

A few of the main features found with this elevated heavy rainfall event was that there was a surface front south of the event and an upper-level area of divergence over and north of the event. Rochette and Moore (1996) also found that there was abundant moisture in the low and middle troposphere near the event area. Their results also did not concur with Colman's (1990) due to the fact that there was a significant amount of CAPE associated with this event, where as in the Colman (1990) cases, there was no CAPE present.

Moore et al. (2003) conducted a study that included twenty-one warm-season heavy rainfall events in the central United States that had developed north of a surface boundary. Storm-relative composites were computed in order to reveal how the environmental conditions of warm-season heavy convective rainfall are associated with elevated thunderstorms. In order for a storm to have been a part of the study it had to meet specific criteria. Elevated thunderstorms must have produced up to 4 inches of rain in a 24 hour period and had to have been initiated or occurring within 4 hours either side of 0000 or 1200 UTC. When analyzing these composites large scale patterns and certain processes were discovered with these events. A few of the results were consistent with

the heavy rain associated with fronts that was described by Maddox et al. (1979) and with Colman's (1990) placement of the elevated thunderstorms.

Moore et al. (2003) found that elevated MCSs were to the north of an east-west-oriented surface front within the cold sector. The MCS was also associated with a region of low-level moisture convergence, which was within the left exit region of the low-level jet (Figure 2.2). The elevated MCS was centered within a divergence maximum that was coupled with the entrance region of the upper-level jet. The main conclusions to the composite results of Moore et al. (2003), were that low-level winds, thermal and moisture fields, resultant advections and regions of forcing are important in determining where elevated thunderstorms will develop and maintain heavy rainfall.

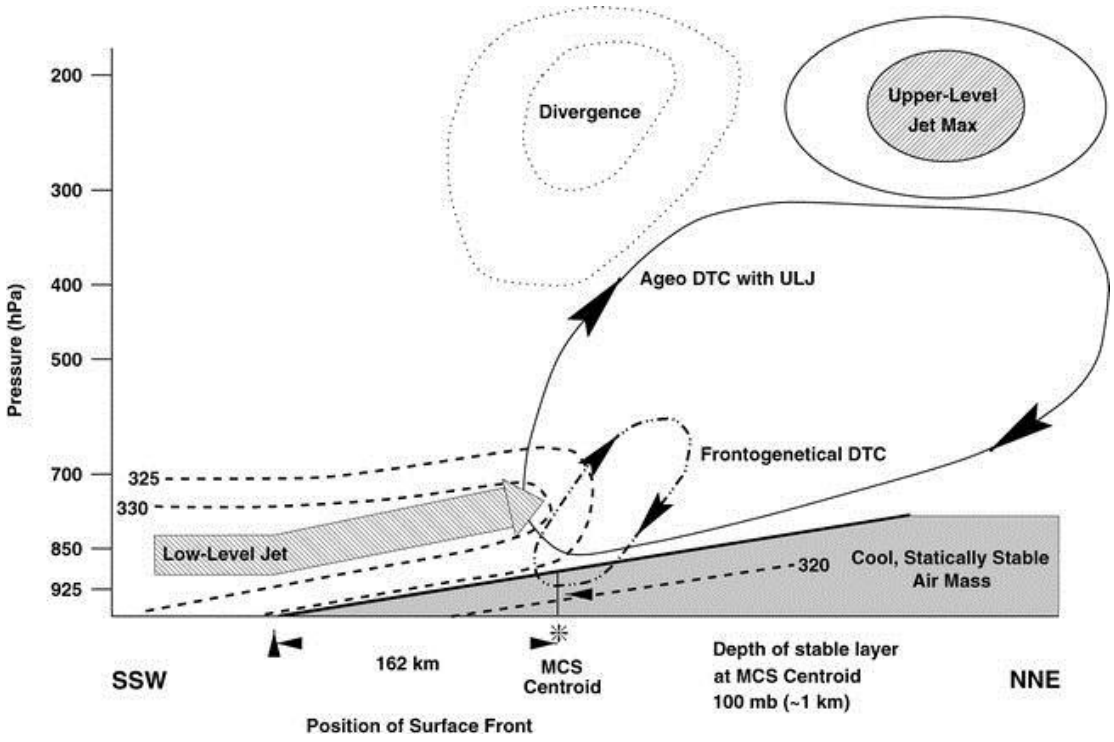


**Figure 2.2. Schematic cross-sectional view taken parallel to the LLJ across the frontal zone. Dashed lines represent typical ue values, the large stippled arrow represents the ascending LLJ, the thin dotted oval represents the ageostrophic direct thermal circulation associated with the upper-level jet streak, and the thick dashed oval represents the direct thermal circulation associated with the low-level frontogenetical forcing. The area aloft enclosed by dotted lines indicates upper-level divergence; the area aloft enclosed by solid lines denotes location of upper-level jet streak. Note that in this cross section the horizontal distance between the MCS and the location of the upper-level jet maximum is not to scale (Image and caption reproduced from Moore et al. (2003)).**

McCoy (2014) created a method to help forecast heavy rainfall produced by elevated thunderstorms in a preferred region for such events in the United States. The study used composite analyses to evaluate the synoptic and mesoscale environments that are associated with heavy rainfall produced by elevated thunderstorms. McCoy found that certain parameters were more prominent indicators of heavy rainfall development over a low-level stable layer. The results of this study are similar to Moore et al. (2003). A few main ingredients that lead to the development of elevated thunderstorms included an

upper-level jet to the northeast of the event, which was associated with the right entrance region and divergence aloft. There was also sufficient environmental moisture apparent when looking at precipitable water values (McCoy, 2014). Precipitable water values were greater than 1.4 inches (3.6 cm) in all the composites, while higher values were advected into the approaching event, which increased to 1.6 inches (4.1 cm) by the time of the event.

McCoy (2014) found the K-index was one of the best forecasting parameters for elevated instability. There were consistent K-index values greater than 35 throughout all the composites, which showed minimal spread in the magnitude or location. Despite MUCAPE being a well known instability parameter, McCoy's composite results showed that MUCAPE has greater spread 6 to 12 hours prior to the event and increased to greater than the mean value (1500 $Jkg^{-1}$) at the time of the event. These parameters were used to analyze two different cases with elevated thunderstorms with heavy rainfall in two different county warning areas (CWA's).

McCoy's (2014) conclusions showed that there were unique patterns that aided in forecasting heavy rainfall production with elevated thunderstorms. A few of theses patterns showed a strong signal but great variability, which consisted of the upper-level jet streak to the northeast of the region and the low-level jet signal from the south-southwest. The K-index (greater than 30) and precipitable water (greater than 1.6 inches) showed strong signals and small variability throughout McCoy's (2014) composites. Figure 2.3 shows where an event should be when combining the K-index, precipitable water, and divergence.

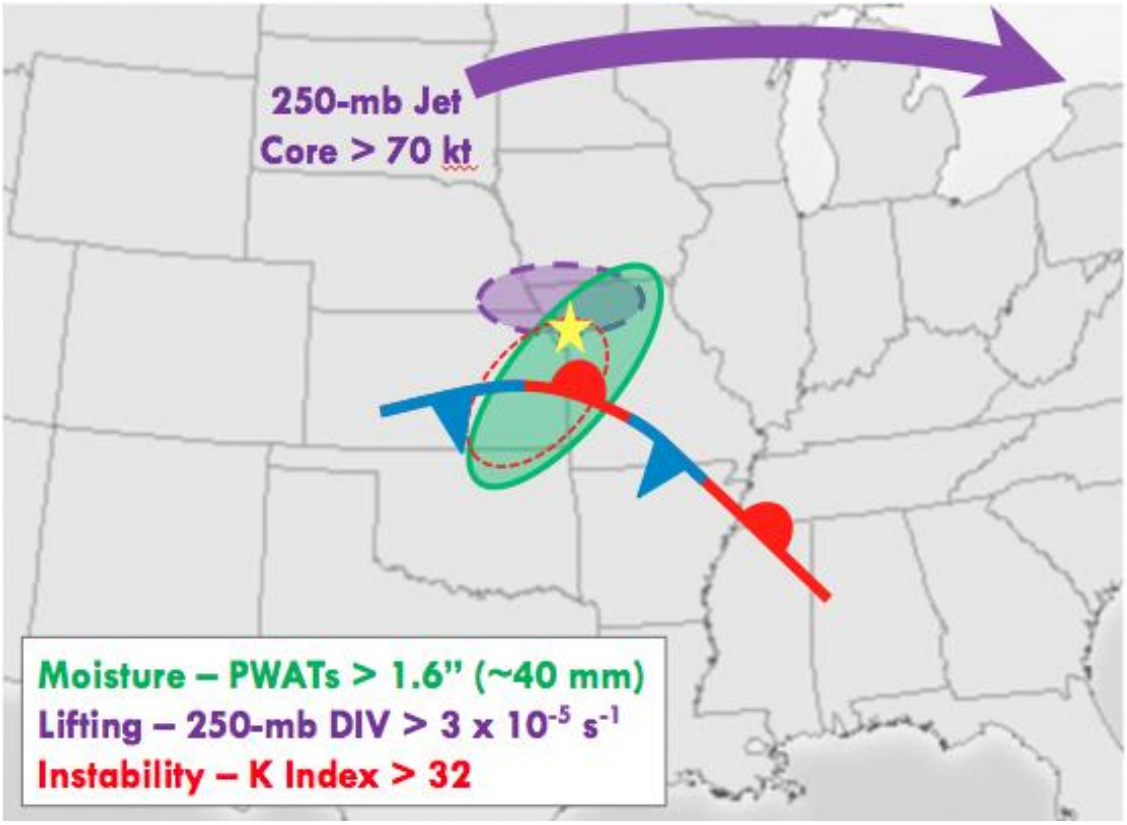


**Figure 2.3. Composite chart of typical location for an elevated thunderstorm, based on the K-index (red; short, dashed oval), precipitable water (green; solid oval), and divergence (purple; thick, dashed oval).**

## 2.3 Flash Flood Forecasting

Maddox et al. (1979) studied 150 events that were linked to intense convective precipitation that caused flash flooding in the central and eastern United States. These events were analyzed by using surface charts and standard level upper-air data. Maddox et al. (1979) identified three basic meteorological patterns that were associated with flash flooding in the central and eastern United States. These patterns were synoptic type events, frontal events, and meso-high events. Maddox et al. (1979) separated events in the western United States into their own category. Even though there is large variability

that can be associated with the meteorological patterns and parameters of forecasting flash flood events, there are still a number of features that are common with each event.

Maddox et al. (1979) found that meso-high and frontal events were mostly nocturnal. Another common characteristics that was observed heavy precipitation typically lasted less than 6 hours. They also found that the frontal events had a maximum occurrence during the month of July (Figure 2.4). Regardless of the type of flash flood event, Maddox et al. (1979) found the following common characteristics:

- Heavy rainfall was produced by convective storms.
- Surface dewpoint temperatures were very high.
- Large moisture contents were present throughout a deep tropospheric layer.
- Vertical wind shear was weak to moderate through the cloud depth.

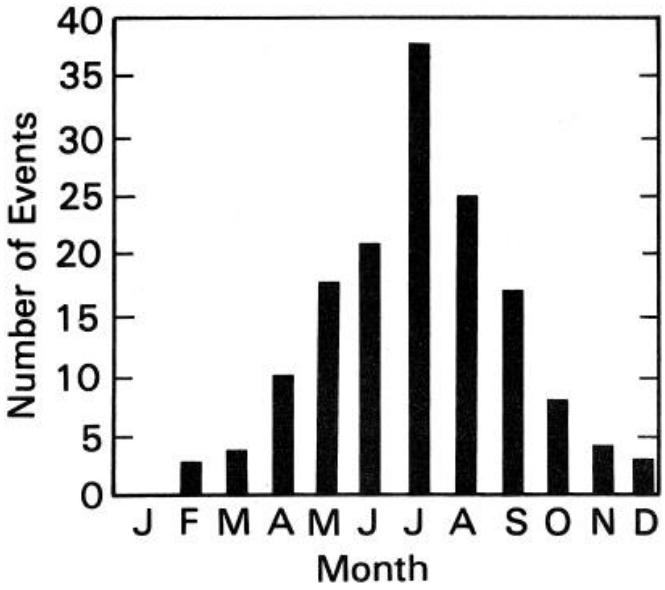


**Figure 2.4. Monthly distribution of flash flood events studied (Image and caption reproduced from Maddox et al. (1979)).**

Despite the complications that can occur when forecasting heavy rainfall events and flash flooding especially due to nocturnal nature of these events, Maddox et al. (1979) was still able to distinguish common characteristics and conditions for these events.

Later, the Doswell et al. (1996) research on flash flooding examined forecasting the potential for it by using an ingredients-based methodology. This research suggests that many flash flood events share a few basic ingredients. A main ingredient for flash flooding is high precipitation rates (Doswell et al.1996). By lifting moist air to condensation the rising air must already have substantial water vapor content and a rapid ascent rate. Doswell et al. (1996) suggested that the there will be low precipitation efficiency while there is high water vapor content and/or vertical motion. Heavy precipitation may occur in a place where the proper hydrological ingredients reside, which in turn will cause flash flooding. Doswell et al. (1996) showed that the ingredients that are associated with flash flooding could be related with deep, moist convection. A few ingredients in order for deep, moist convection to occur has mostly to do with buoyancy. To produce buoyancy and deep convection the environmental lapse rate must be conditionally unstable, sufficient moisture should be available, and there must be a lifting mechanism to lift the parcel to the level of free convection (LFC) (Doswell et al.,1996). They stated "an ingredients-based methodology is a logical choice for the application of scientific understanding to the forecasting task". By using these critical ingredients and observations together, a forecaster can reduce their choices in making a forecast and can focus on the task at hand.

Doswell et al. (1996) state that the anticipation of a possible flash flood event is critical in handling the situation properly in practice. The processes on various scales that

lead up to the flash flood event are described by Doswell et al. (1996) as large scale processes, mesoscale processes, storm-scale processes, and forecasting meteorological processes. They believe that if the synoptic and mesoscale processes present the right ingredients, then a flash flood event can occur. In order for a forecaster to be able to determine whether ingredients, such as high precipitation rates and buoyancy exist for an event to produce heavy rainfall, the forecaster must be educated and trained on such events.

Schumacher and Johnson (2006) believe that ingredients are necessary to identify forecasting flash flooding, but suggest that there are different challenges involved when forecasting rainfall associated with a strongly forced system. Schumacher and Johnson (2006) study focused on characteristics of flash floods, such as Doswell et al (1996), but concentrated on radar-indicated structures of systems and common patterns with MCSs. Schumacher and Johnson (2006) conducted a study that examined many features of extreme rain events in the United States over a 5-year period. They defined an extreme rain event when one or more of the stations reported 24-hour rainfall rate greater than the 50-year occurrence, of which 184 events were considered extreme rain events after eliminating bad rainfall reports. One of the main foci of this study was to observe the variation of extreme rainfall monthly frequency distributions. It was found that many of these events were associated with the warm season especially in the Plains region of the United States; commonly in June and July (Figure 2.5). Events that were more frequent in March, August, and September were more to the northeast.

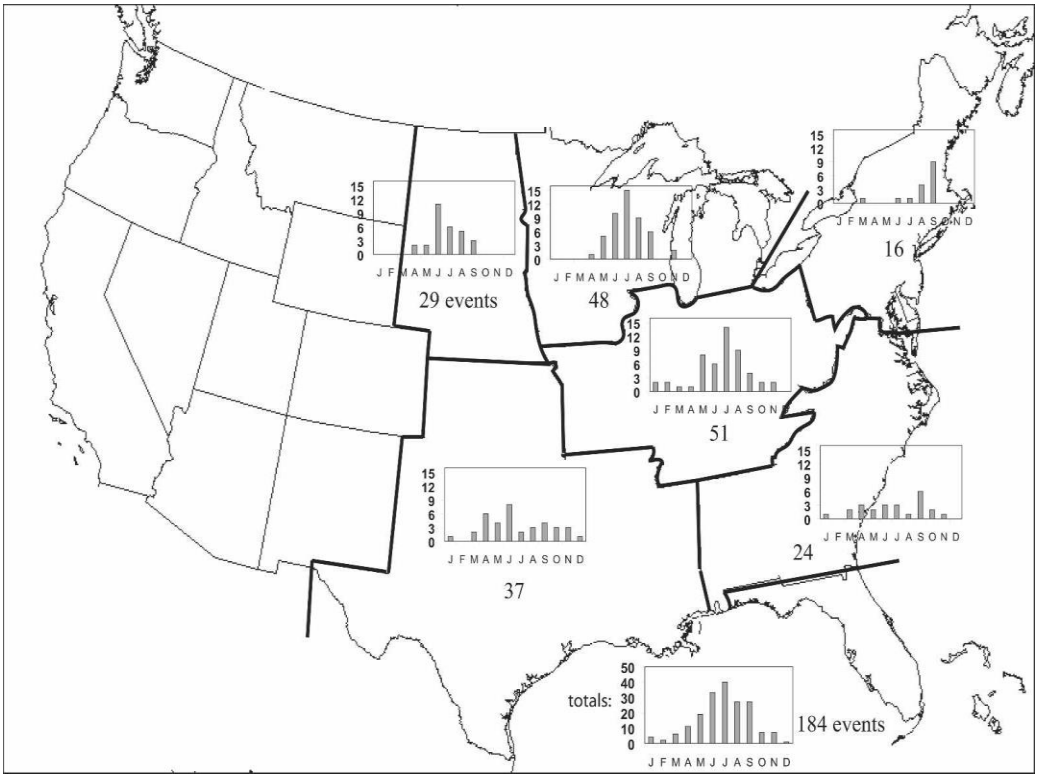


**Figure 2.5. Shows the monthly frequency distribution of extreme rain events for 7 different regions (Image reproduced from Schumacher and Johnson, 2006).**

Many of Schumacher and Johnson (2006) results were similar to Maddox et al. (1979) results in identifying storm systems that produced heavy rainfall and flash flooding. These events occurred in the late afternoon and evening, which means that they peaked after dark and dissipated or moved out of the area in the early morning hours (Schumacher and Johnson, 2006). One of the main patterns that Schumacher and Johnson (2006) found was during frontal events, where a convective line formed on the cool side of and parallel to a pre-existing slow moving synoptic boundary. Frontal events were found to occur more frequently during the warm season. Schumacher and Johnson (2006) study found that the majority of the extreme rain events were more frequent in the

month of July. A main conclusion noted by Schumacher and Johnson (2006) was approximately 90% of extreme rain events were associated with flash flooding.

## 2.4 Elevated Severe Thunderstorms

Grant (1995) conducted a preliminary study on elevated thunderstorms by collecting upper-air soundings, surface data, and model gridded data for eleven cases from April 1992 to April 1994. He based the selection of severe thunderstorms off of the criteria from Colman (1990) to determine whether or not those storms were elevated. Thunderstorms that developed in the cold sector north of a surface front were found embedded in a layer above a significant and shallow frontal inversion (Grant, 1995).

By looking at soundings in or near the area of these storms Grant (1995) found that the most unstable parcels frequently occurred near the 850-hPa level. The soundings also showed strong warm air advection profiles above the 500-hPa level. Areas of strongest upward motion and destabilization occurred above the boundary layer, which had led to the initiation of severe thunderstorms. Stability indices are commonly used to help forecast severe thunderstorms and the degree of instability. Grant (1995) found that even though surface conditions were cool and stable, stability indices suggested that a marginal degree of instability was required to form a severe thunderstorm in the cold sector. He also found that there were at least five severe thunderstorm reports near the location of the event at least 50 statute miles north of the boundary.

## 2.5 Indices

Doswell and Schultz (2006) discussed how diagnostic variables are used properly (and improperly) when severe-storm forecasting. Meteorologists refer to many diagnostic variables as forecast parameters. A few forecast parameters have been associated with aiding in forecasting severe convection and forecasts are being based on those variables. Doswell and Schultz (2006) suggest that diagnostic variables be used when assessing qualitatively the state of the atmosphere at the time of their calculation and are not useful for future weather. They do believe that some forecast parameters could be accurate for forecasting short periods that are close to their diagnosis. It is known to most meteorologists that a forecast parameter should not be the only data used for a forecast, especially for severe weather. Doswell and Schultz (2006) suggest that an ingredient based forecasting method, such as Doswell et al. (1996), is more beneficial in operational forecasting.

Doswell and Schultz (2006) described that there are a few requirements that a proper forecast parameter should meet. One way to verify a forecast parameter is by using a contingency table and by choosing a threshold value for the parameter and verifying whether it is within that threshold or not. Once this is done, Doswell and Schultz (2006) suggest testing the skill of the parameter by comparing the accuracy of the anticipated forecast based on the forecast parameter against the accuracy of a standard forecast method, such as climatology. If the forecast parameter shows statistical skill when compared with the standard method, then Doswell and Schultz consider that forecast parameter to be possibly useful for future forecasts.

## 2.6 Forecast Verification

Forecast verification can be defined as the process in which the predicted weather is compared to the actual weather, where the output of this data produces one or more scores or indices. These scores or indices are then compared to some standard, such as climatology, that is dependent on the type of verification that is needed. Verification methods can create objectivity, which eliminates the subjectivity verification that is sometimes created by meteorologists (Panofsky and Brier, 1968). In order to create this objectivity, a forecast verification must be clearly stated at the beginning of the verification process. This will be based on the purpose of the verification since not all verification methods are useful for every research type. Forecast verification, specifically statistics, help provide useful information in how well forecasts are performing and assist forecasters in identifying where blunders could be achieved (Jolliffe & Stephenson, 2003).

There are many different types of categories of forecast verification methods, which include verification measures. Jolliffe and Stephenson (2003) define a verification measure as any function of the forecasts, the observations, or their relationship and includes the probability of the observed event. Verification measures then consist of a subcategory called performance measures. The performance measures put a focus on the similarity between the forecast and observations, which can be collective or individual. Performance measures included hit rate and false alarm ratio (FAR). Hit rate is the proportion of occurrences that were correctly forecast,

$$H = \frac{a}{a+c} \tag{1}$$

where H is the hit rate, a is the number of hits, and c is the number of misses.

Hit rate is also known as probability of detection (POD), which can also be interpreted as a sample estimate of the probability of a forecasted event based on if the event was observed (Jolliffe & Stephenson, 2003). POD is very sensitive to hits while ignoring false alarms. POD answers the question of what fraction of the observed events was correctly forecasted. POD can range from 0 to 1, while a perfect score will have a score of a 1.

False alarm ratio (FAR) is based on the proportion of forecast occurrence that was not followed by an actual occurrence. If the skill of the forecast is perfect, POD=1 and FAR=0. This statistical score is sensitive to false alarms but not misses. FAR answers the question of what fraction of the predicted events actually occurred. FAR ranges from 0 to 1, while a perfect score for FAR will be zero,

$$FAR = \frac{b}{a+b} \tag{2}$$

where FAR is the false alarm ratio, a is the number of hits and b is the number of false alarms.

Another way to verify forecasts is to use a scoring measure. The most widely used performance measure is the critical success index (CSI), which can give a probability of a hit given that the event was either forecasted, or observed, or both. CSI is used most often as a performance measure due to the fact that it can be calculated without the use of the frequency of correct rejections. This is also true for POD and FAR and is often used together because they share this similarity. When there is perfect skill CSI will have a maximum value of 1, while when there is no hits CSI is 0. CSI measures a portion of forecasted events that were correctly predicted,

$$CSI = \frac{b}{a+b+c} \quad (3)$$

where CSI is the critical success index, a is the number of hits, b is the number of false alarms, and c is the number of misses. This score does not indicate skill and is sensitive to hits while penalizing both misses and false alarms.

Table 2-1 is a contingency table, which states what each of the terms in POD, FAR, and CSI equations.

**Table 2-1: A two-way contingency table.**

| Event Forecast | Event observed | | |
|---|---|---|---|
| | Yes | No | Total observed |
| Yes | a (hits) | b (false alarms) | a + b |
| No | c (misses) | d (correct rejections) | c + d |
| Total | a + c | b + d | a + b + c + d = n |

The correlation coefficient measures the association between the forecast and observations independent of the mean and variance of the marginal distribution (Jolliffe & Stephenson, 2003). The values of correlation coefficient ranges from -1 to +1, with +1 being a perfect positive relationship and -1 being a perfect negative relationship.

# Chapter 3. Methodology

## 3.1 EPEC Calculation

EPEC has been used as part of a research project called Program for Research on Elevated Convection with Intense Precipitation (PRECIP). EPEC involves three parameters: K-index (KINX), 250-hPa divergence ($Div_{250}$), and precipitable water (PWAT) (Equation 4). K-index is unitless, precipitable water is in millimeters, and divergence is in $s^{-1}$, which is scaled due to it being smaller than K-index and precipitable water. EPEC is unitless.

$$\underset{}{EPEC} = \underset{}{KINX} + \underset{mm}{PWAT} + (\underset{s^{-1}}{Div_{250}} \times 100{,}000) \quad (4)$$

Units are neglected in the formation of EPEC.

These three parameters were shown to have strong signal and low variability using interquartile range (IQR) through McCoy's (2014) composites. McCoy's composites also showed that the K-index (a proxy for instability) increased with time leading up to heavy rainfall with elevated convection. IQR plots of the K-index indicated that the K-index performs better at analyzing the increase of elevated instability. Precipitable water is the moisture variable, which behaved much like the K-index. The large IQR of 250-hPa divergence shown through McCoy's composites was larger than for the K-index or precipitable water, but divergence was still the best of the proxy variables

**Table 3-1. Values employed from McCoy (2014) to assemble the EPEC Index percentile values. K-index (KINX) is unitless, precipitable water (PW) is in millimeters, and divergence (DIV) is the 250-hPa value scaled up by $10^5$ with units of $s^{-1}$. Even so, EPEC is treated as a unitless number. Also the EPEC mean and standard deviation calculated directly from reanalysis of the probability distribution function of the original 60 EAX soundings in McCoy (2014).**

| | KINX | PW | DIV | EPEC |
|---|---|---|---|---|
| 25th percentile | 33 | 40 | 2 | 74 |
| 50th percentile | 35 | 46 | 5 | 86 |
| 75th percentile | 37 | 51 | 8 | 96 |
| | | | | |
| 1 SD below | | | | 83 |
| Mean | | | | 89 |
| 1 SD Above | | | | 98 |

for suggesting lift. Despite the large variability, 250-hPa divergence still showed strong signal for the events.

EPEC threshold values are based upon the 25th, 50th, and 75th percentiles from composite statistics, shown in Table 3-1. These numbers come from McCoy's (2014) thesis for each of the three parameters used to calculate EPEC, and assumed a normal and even distribution about the 50th percentile. (This approach guided foprecast operations in late 2014 and 2015.) Also included in Table 3-1 are the mean and standard deviation values from the sixty (60) Pleasant Hill (EAX) county warning area soundings studied by McCoy (2014), which are offered here in this way for the first time. These latter values will be used later for a comparison to climatology.

Based upon this work, EPEC can only be employed reliably on the cold side of the $\Theta_e$ boundary, which has been associated with where the initiation of elevated convection occurs.

## 3.2 Event Selection

The goal of this project is to verify if the parameter EPEC can be used as a predictive measure for forecasting heavy rainfall. In order to analyze how EPEC performs with forecasting heavy rainfall, events were collected from the PRECIP project dataset, which incorporates the states of Kansas, Missouri, Iowa, Nebraska, and Oklahoma (Figure 3.1). Also, this period exists outside the timeframe of McCoy (2014). Events were chosen based on whether they met the deployment criteria set by the PRECIP team. Table 3-2 shows the events for which the PRECIP team deployed or recorded for future research. The latter group of events were missed events (did/could not deploy PRECIP personnel).

## 3.3 Data

Several datasets were employed to accomplish the subjective and objective verifications. For subjective rankings, the precipitation field was used derived from the NEXRCOMP storm total precipitation (STP) product, which is on a 4 km grid. Then, both the North American Model (NAM) and Global Forecast System (GFS) were used to plot the EPEC index, which are plotted on a 80 km grid. This was not to discriminate or

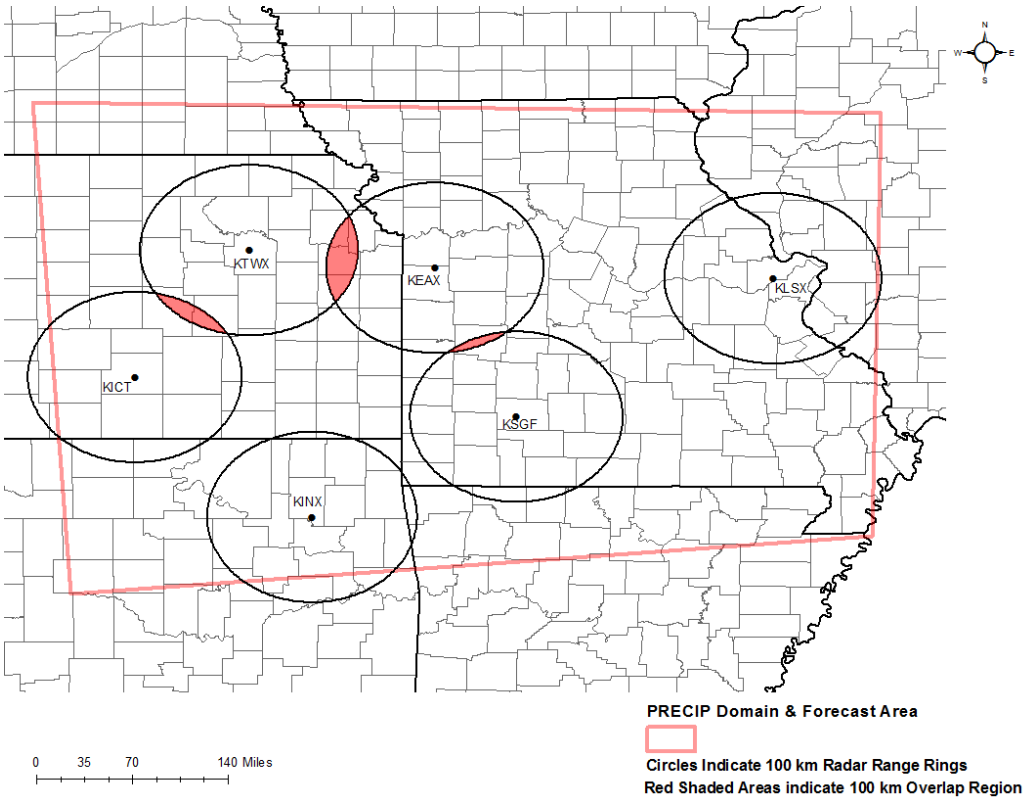


**Figure 3.1 Zoomed plot of study area (eastern Kansas and western Missouri) and several of the NWS WSR-88D Doppler radar sites in the region with range circles every 100 km: Topeka, Kansas (TWX); Pleasant Hill, Missouri (EAX); Springfield, Missouri (SGF); Tulsa, Oklahoma (KINX); Wichita, Kansas (KICT); and also St. Louis, MO (KLSX). Red shading indicates regions where radars overlap at 100 km. (Image and caption reproduced from the PRECIP site).**

rank the models because each event when initially forecasted by the PRECIP project used both models.

For the objective verification work, The EPEC index was calculated using the initial Rapid Refresh (RAP) 130 and/or RAP 236. Only two events used the RAP 236 due to RAP 130 data not being available for 07 July 2014 and 17 July 2014. The RAP 236 was also used for the synoptic analysis of the example of the worst and best case for EPEC. The precipitation data used is called Precipitation NCEP/ EMC 4 km Gridded

**Table 3-2: Table that shows the date and location of the 15 elevated convection events that the PRECIP team either deployed on or recorded for future analysis. Deployment events are bold.**

| Date | Location |
|---|---|
| **20140402** | **W MO** |
| 20140511 | SE NE |
| **20140604** | **S IA / N MO** |
| **20140607** | **S KS** |
| 20140710 | S KS |
| **20140717** | **C OK** |
| 20140807 | C MO |
| 20140827 | NW MO |
| 20150403 | E MO |
| **20150605** | **NW MO** |
| **20150611** | **E NE** |
| **20150625** | **E IA** |
| **20150708** | **C MO** |
| 20150716 | SW IA/NW MO |
| 20150730 | C KS |

Data (GRIB) Stage IV data from the NCAR UCAR Earth Observing Laboratory site[1]. This Stage IV precipitation was downloaded and plotted with the EPEC index in order to verify if EPEC could aid in forecasting for heavy precipitation associated with elevated thunderstorms. Bi-linear interpolation was used in gempak, known as gdbiint, to convert the 4 km precipitation to a 13 km grid for the RAP 130. For the 2 events that used the RAP 236, the precipitation data was interpolated up to 40 km.

In order to estimate a climatological EPEC value, 60 years of precipitable water values were obtained for Topeka, KS, which is closest to the Pleasant Hill county warming area. From these, mean, standard deviation, and percentile values were constructed.

[1] Site from which Stage IV precipitation were downloaded: http://data.eol.ucar.edu/codiac/dss/id=21.093

## 3.4 Verification

The events in question were studied subjectively (ranking) and objectively (direct statistical comparison of EPEC to ensuing 6-hour precipitation). Additionally, we have calculated EPEC for the original 60 soundings for the Pleasant Hill county warning area in order to create a statistical distribution that we can compare to climatology. This will allow us to establish a baseline for EPEC performance.

### 3.4.1 Subjective Event Rankings

Once the events were analyzed, the initial analysis ranked them based on where the maximum storm total precipitation occurred, and the 30- to 36-hour lead-time forecasted EPEC values were based upon precipitation. Ranking these events was the initial subjective approach to this research but produced some interesting results. This approach helped to assess how well EPEC would be as a predictive tool with heavy precipitation, as EPEC was used when the PRECIP project forecasted for heavy rainfall associated with elevated convection.

The rankings were based on how well EPEC performed relative to where the maximum storm total precipitation occurred. The range of the rankings is from 0-3, in which 0 being the worst and 3 is where EPEC represented the event very well. Table 3-3 shows the descriptions of what each ranking value represents.

**Table 3-3. Table describing the rankings of events and associated to how EPEC forecasted for the heavy rainfall.**

| Rankings | Description |
|---|---|
| 0 | Complete miss |
| 1 | Marginal guidance |
| 2 | Good/Useful forecast |
| 3 | ‘Epic', highlights correct region |

## 3.4.2 Objective Event Verification

There were 21 cases that were recorded by the PRECIP team but needed further analysis to determine if the events truly occurred north of a boundary, over the cold sector. Comparing where the 6-hour precipitation occurred to where the archived surface front was analyzed by the Weather Prediction Center showed which cases were elevated. By performing this comparison, 6 cases were eliminated based on the position of the heavy rainfall relative to the analyzed surface front. Table 3-2 shows the 15 cases that were analyzed to be elevated based on precipitation and the surface front.

The correlation coefficient of EPEC and ensuing precipitation was calculated for each of the 15 elevated thunderstorms with heavy rainfall cases. Geographical pairs of RAP130 EPEC (on a 13-km grid) and the NCEP Stage IV precipitation data for the ensuing 6-hour period (interpolated from 4-km to the RAP 130 13-km grid) greater than 0.5 inches (12.7 mm) were formed; these values were then run through a program called ProStat. The correlation coefficient determined whether there is a positive or negative relationship between EPEC and the precipitation.

Additionally, EPEC was verified by calculating statistics using a small piece of FORTRAN code, which calculated the forecast verification statistics probability of detection (POD), false alarm ratio (FAR), and critical success index (CSI). Looking back

at Chapter 2, these verification methods were used because they are known as performance measures, which uses hits, misses and false alarms. These methods will help verify whether EPEC can be considered a forecast parameter that can be useful for future forecasts (Doswell and Schultz, 2006).

This code read through the precipitation file and EPEC file as a pair. Every precipitation value greater than 12.7 mm (0.5 inch) in 6 hours was selected. The FORTRAN code put a threshold on the EPEC, which will the $25^{th}$ percentile or 74 and the precipitation threshold is 12.7 mm (0.5 inches), the latter is a simple linear scaling of McCoy's (2014) threshold of 50.8 mm (2 inches) in 24 hours. These values were then used to calculate POD, FAR, CSI and the bias. Then each forecast verification statistic was calculated inside the code and then printed out with each statistic value.

Analysis images were created for EPEC and the 6-hourly Stage IV data form NCEP through GEMPAK. EPEC is plotted for the beginning of the 6-hour time period over which the precipitation accumulates. The data used to calculate EPEC was from the RAP 130 or 236 models. An example of this format is shown in Figure 3.2.

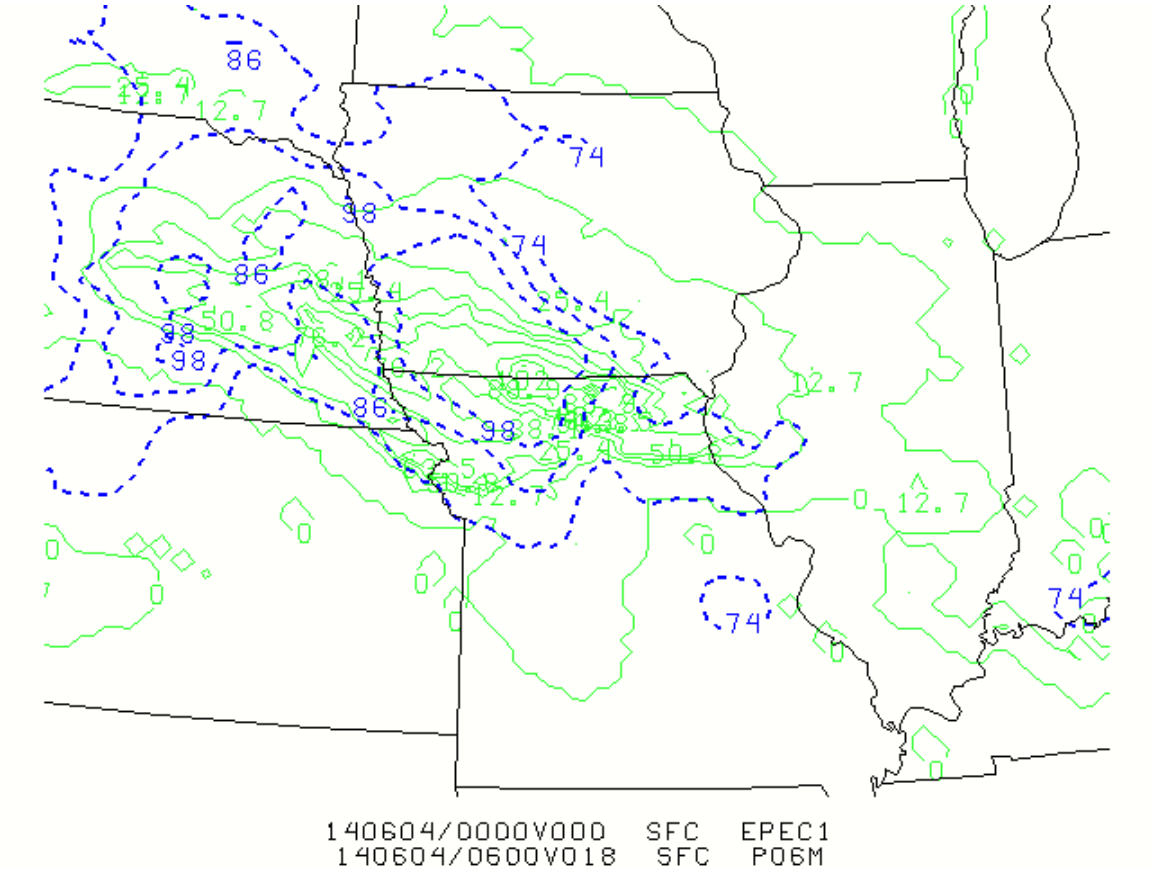


**Figure 3.2. Example of the image created using GEMPAK with RAP 130 EPEC values (dashed, blue) and 6-hourly stage IV precipitation data (solid; every 0.5 inches [12.7 mm]).**

## 3.4.3 Test Against Climatology

In an effort to assess further the utility of the EPEC tool as a forecast parameter for elevated heavy rainfall, it was compared to climatology, as alluded to in Doswell and Schultz (2006). As such, climatological values for the K-index from the Plains states (DeRubertis, 2006) and average precipitable water values from Topeka, Kansas (Storm Prediction Center, 2016), were determined for the Midwestern region where McCoy (2014) derived her composites. Coupled with the assumption that divergence on the average day is ~ 0, sufficient values exist in order to estimate a climatological EPEC value.

Two seasonal calculations were made: one for spring (March, April, and May), and one for summer (June, July, and August) following results in DeRubertis (2006). For the K-index, DeRubertis (2006) provides a mean for the Plains region (Figure 3.3), as well as a first standard deviation. For the precipitable water, the Storm Prediction Center (2016) data allows for calculation of corresponding mean and standard deviation values, which were completed though only for Topeka, KS, which is near the latitudinal midpoint of DeRubertis'(2006) Plains region. With these values, we can also evaluate at the upper reaches of the normal atmospheric condition (i.e., normal rainfall situations).

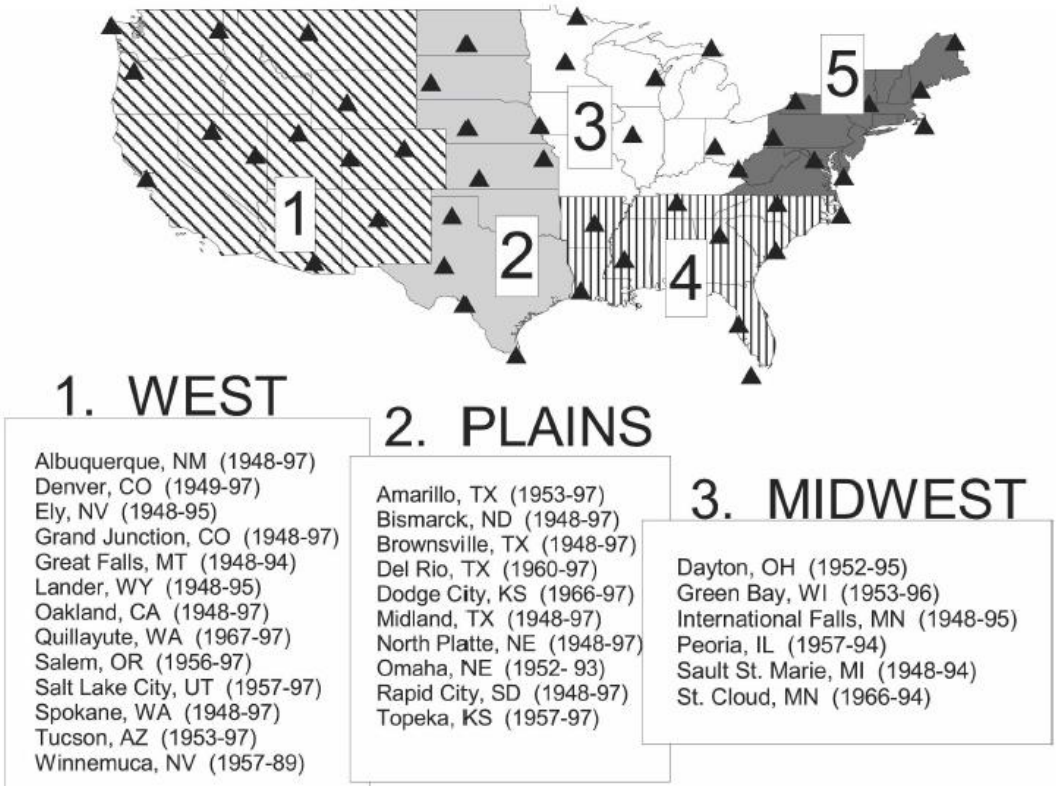


**Figure 3.3. Region 2 represents where DeRubertis (2006) considers the Plains with associated radiosonde stations (Image reproduced from DeRubertis (2006).**

## 3.5 Why the K-index?

Of all of the variables tested, K-index had an excellent signal in its mean field, and one of the lowest interquartile ranges. This result derives directly from the work of McCoy (2014).

Although it is true that the K-index is an empirical, non-derived parameter (Doswell and Schultz 2006), it has been used widely for decades, because of its rational physical underpinnings. Increased low-level (850-hPa) temperatures and dew points tends to suggest decreasing static stability, and will also drive the K-index up. Likewise, decreased upper-level (500-hPa) temperatures also suggest decreasing static stability, and will also produce higher values of K-index. Meanwhile, a decreased dew point depression at 700 hPa suggests low- to mid-level moistening, which also serves to drive the K-index up. Each of these changes demonstrates a moistening, destabilizing atmosphere, increasingly suitable to support convection. This sound physical reasoning for the K-index has not changed since its introduction by George (1960).

# Chapter 4: Results

In the chapter the examination of the results of the initial subjective ranking study and then proceed directly to the objective verification statistics. Afterwards, the cases where the EPEC values performed best, and worst are looked at.

## 4.1. Rankings

The goal of this subjective analysis was to verify whether EPEC could predict where the heaviest rainfall occurred. Both the NAM and the GFS were examined for each event and ranked accordingly. Each model was used during the PRECIP project and a model of the day was chosen for each event based on how well the model performed through previous forecasts for which the lead forecaster had high confidence in.

The initial approach to verify if EPEC can be a predictive parameter was to rank all 15 events archived by the PRECIP project in 2014 and 2015, while only being employed on the cold side of the $\Theta_e$ boundary. The events were ranked based on how well EPEC identified where the maximum storm total precipitation (STP) occurred. The first step was to use the North American Model (NAM) and/or the Global Forecast System (GFS) models to plot EPEC and the heavy rainfall. Radar composite storm total precipitation (STP) was plotted at the time where the maximum rainfall occurred for the event. The EPEC index was plotted for the model time prior to the occurrence of the maximum rainfall, which was often 36 hours into the run.

A numerical value of 0, 1, 2, or 3 was assigned subjectively to each event, with 0 being the worst and 3 being the best. Table 3-3 shows the descriptions of what each

ranking value represents. These values were applied to each event based on how well EPEC captured where the heavy rainfall occurred.

There was one event that was ranked as a 0, while there was a total of eight events ranked as a 3. A total of 8 deployments occurred where the PRECIP team conducted observations in the field and the majority of these IOP's were ranked as a 2 or a 3. EPEC was used during the PRECIP project to determine whether a deployment should occur and these rankings show that EPEC did perform quite well when a deployment occurred. Table 4-1 shows the distributions of the rankings of each event. The bold values indicate the examples of each of the rankings and will be discussed below.

**Table 4-1: Table listing the 15 elevated events with the location of events and their associated rankings from the GFS and the NAM. Bold events are the associated examples of each ranking.**

| Date | Location | IOP | GFS-36hr | NAM-36hr |
|---|---|---|---|---|
| **20140402** | **W MO** | **1** | **0** | 2 |
| 20140510 | N MO | | 0 | 1 |
| 20140604 | S IA / N MO | 2 | 1 | 2 |
| 20140607 | S KS | 3 | 3 | 1 |
| 20140710 | S KS | | 2 | 2 |
| **20140717** | **C OK** | **4** | **3** | 2 |
| 20140807 | C MO | | 3 | 3 |
| 20140827 | NW MO | | 3 | 2 |
| 20150403 | E MO | | 1 | 1 |
| 20150605 | NW MO | 5 | 3 | 2 |
| 20150611 | E NE | 6 | 2 | 2 |
| **20150625** | **E IA** | **7** | **1** | 1 |
| 20150708 | C MO | 8 | 3 | 3 |
| **20150716** | **SW IA/NW MO** | | 2 | **2** |
| 20150730 | C KS | | 2 | 2 |

The following figures are examples of each set of the type of rankings, which are 0, 1, 2, and 3. The focus of each plot is based on where the maximum amount of rainfall occurred with that event and where EPEC forecasted for the event.

Figure 4.1 shows an event that occurred on 02 April 2014 in western Missouri. This event is also known as IOP 1, where a PRECIP team conducted observations in Ozark and Clinton, Missouri. This event was ranked as a 0 using the Global Forecast System (GFS). Rainfall totals in western Missouri were less than 2 inches for this event. Figure 4.1 shows that the majority of the rainfall occurred through central Missouri, while there are no EPEC contours to highlight any of the rainfall. IOP 1 was ranked as a 0 based on EPEC not forecasting this rainfall event 36 hours prior to the actual occurrence. EPEC may have missed this event due to low precipitable water values.

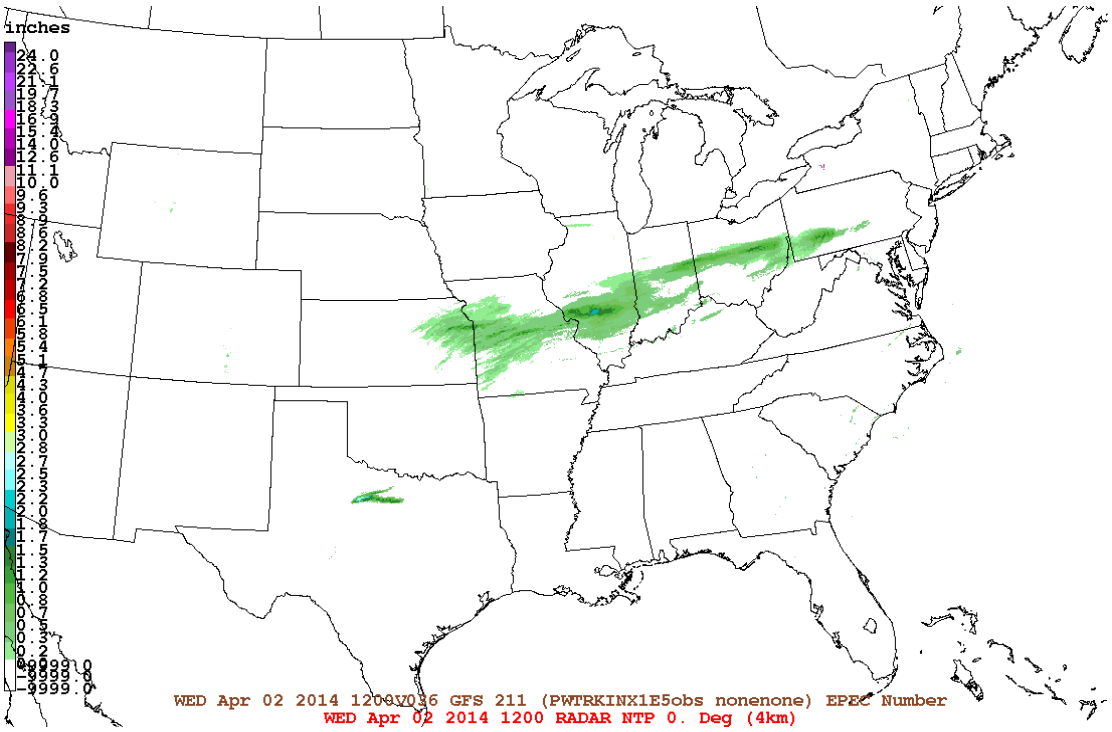


**Figure 4.1. Example ranking of a 0 on 02 April 2014 for an event that occurred in western Missouri with storm total precipitation (color-filled) and EPEC (solid brown) using the thinned GFS, 80-km model output. Scale on the left defines precipitation amounts.**

The event of 25 June 2015 (Fig. 4.2) occurred in eastern and central Iowa. The PRECIP project went out on a deployment with this heavy rainfall event, which is known as IOP 7, and conducted observations in Iowa City and Bloomfield, Iowa. Heavy rainfall amounts between 76 and 178 mm (3 and 7 inches) occurred within parts of Iowa and Missouri. The EPEC index did highlight a portion of the heavy rainfall event but only the edge of the contours while the maximum values of EPEC were well off to the east in northeast Illinois. Despite EPEC highlighting part of the heavy rainfall, this event was ranked as a 1 using the GFS, due to the eastward displacement of the maximum EPEC contours.

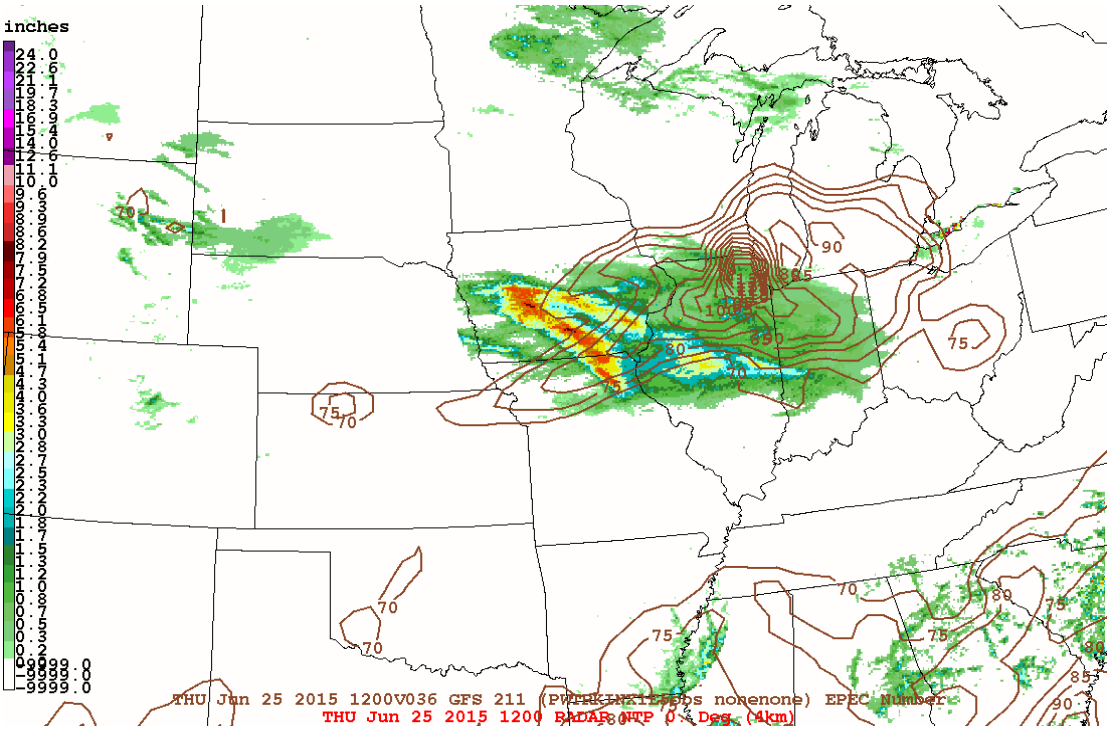


**Figure 4.2. Example ranking of a 1 on 25 June 2015 for an event that occurred in eastern and central Iowa; format as in Fig. 4.1.**

The event that occurred on 16 July 2015 in northwestern Missouri is shown in Figure 4.3. During this event there were STP values from 3 to 8 inches that accumulated with this heavy rainfall event. The EPEC index highlighted this area of heavy rainfall with contour values greater than the 50$^{th}$ percentile, which is an EPEC value of 86. A maximum EPEC value of 90 is present but is to the east of where the actual event occurred. Despite EPEC values highlighting the event with values greater than the 50$^{th}$ percentile, this event was ranked as a 2 due to the displaced EPEC maxima using the NAM 211.

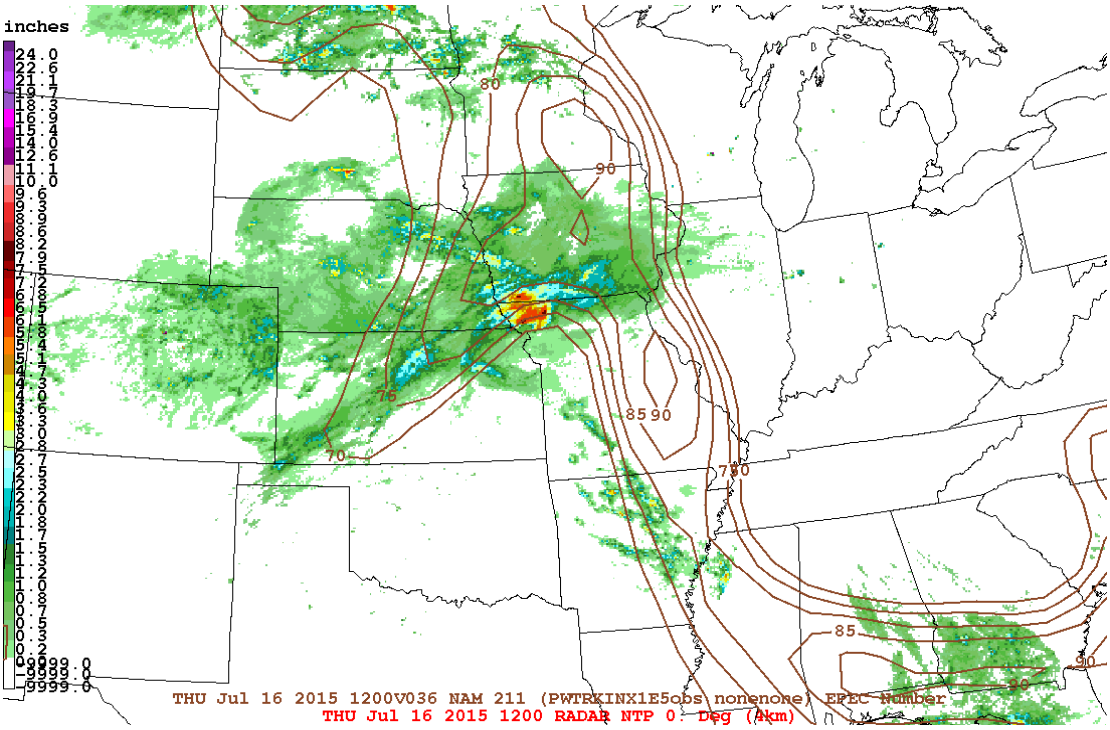


**Figure 4.3. Example ranking of a 2 on 16 July 2015 for an event that occurred in northwestern Missouri; format as in Fig. 4.1.**

On 17 July 2014 a heavy rainfall event occurred in central Oklahoma, shown in Figure 4.4. STP values for this event were as high as 203 mm (8 inches) for the heavy rainfall occurrence. EPEC index contours highlight the entirety of the rainfall event with values greater than the 75$^{th}$ percentile, which is an EPEC value of 98. Even though the maximum EPEC value of 110 is slightly to the northeast of the heavy rainfall this event was ranked as a 3. The orientation and shape of the EPEC contours shows the shape of where the heavy precipitation occurred. This reason why this event was ranked as a 3 is due EPEC highlighting the entirety of the event with values greater than the 75$^{th}$ percentile.

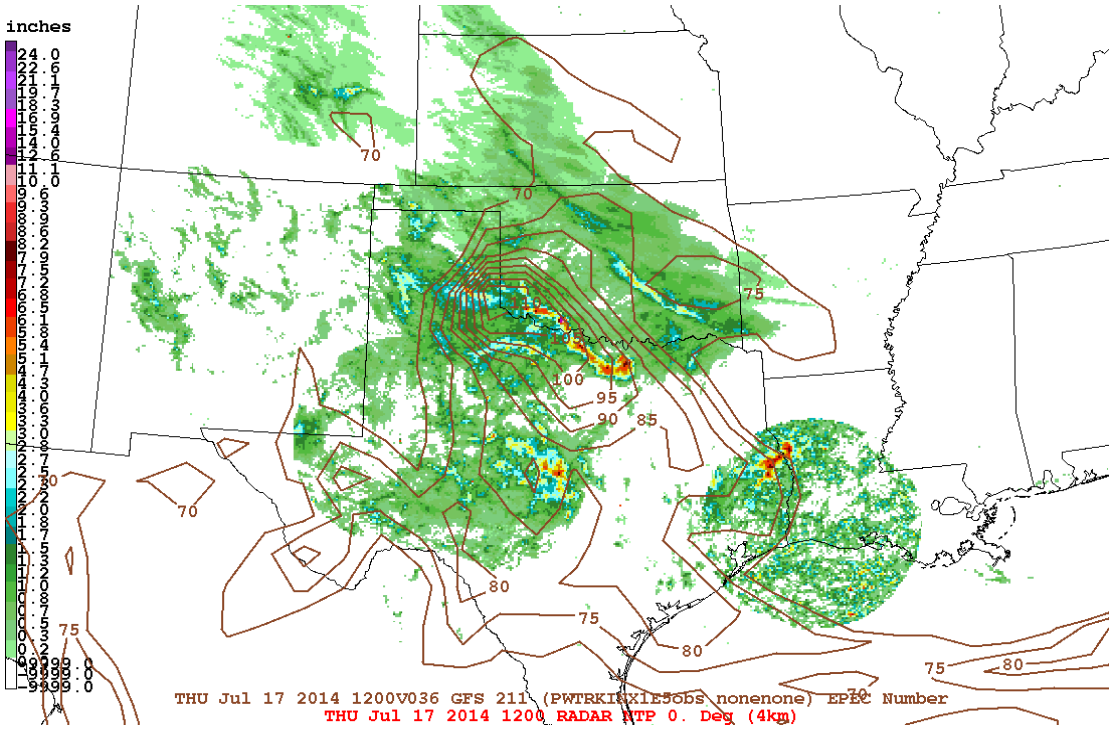


**Figure 4.4. Example ranking of a 3 on 17 July 2014 for an event that occurred in central Oklahoma; format as in Fig. 4.1.**

The initial analysis of this research was to rank the 15 heavy rainfall events associated with elevated convection according to how EPEC forecasted the rainfall 36 hours prior to the event occurrence. This analysis was designed to show how well EPEC would do based on a subjective point system, and how EPEC was used during 2014 to 2015 with the Program of Research on Elevated Convection with Intense Precipitation. Based on the rankings in Table 4-1, the majority of the events were higher ranked, while IOP's were mostly 2 or 3's. There was only a single event ranked as a 0 based on the GFS. These results showed that EPEC could help identify areas of heavy precipitation, while being employed on the cold side of the $\Theta_e$ boundary.

## 4.2. Statistical Analysis

These statistical analysis results were based on the 15 elevated cases that were verified to be north of a boundary and/or found in the cold sector. Each case was processed through PROSTAT and a FORTRAN program to produce these statistical values of correlation coefficient, probability of detection (POD), false alarm ratio (FAR), critical success index (CSI), and bias.

The correlation coefficients for each of the 15 elevated thunderstorms with heavy rainfall cases are shown in Table 4-2. In Table 4-2, there is a column that states the number of degrees of freedom associated with the 15 events. The number of degrees of freedom is the number of values of EPEC with 6-hour precipitation used for the calculations of the 3 statistics. A threshold of 30 degrees of freedom was placed on each of the events in order to exclude cases with low values. Only one event had a value less than 30. This suggests that all the values in Table 4-2 are statistically significant. Nine cases show a probability matrix less than 0.05, while the correlation coefficient values associated show a positive (even if weak) positive relationship between EPEC and ensuing 6-hourly precipitation totals, suggesting that as precipitation increases so should EPEC.

**Table 4-2: Events and associated values of correlation coefficient between 6-hour precipitation totals and EPEC, probability matrix, z-value matrix, and degrees of freedom. Bold numbers are the significant values discussed in Chapter 4 and the red italicized values are events that used the 40-km RUC.**

| Date | IOP | Corr Coef | Prob Matrix | z-value Matrix | DOF |
|---|---|---|---|---|---|
| 2014040206 | 1 | 0.0427 | 0.6364 | 0.0427 | 123 |
| 2014051018 | -- | -0.0554 | 0.7179 | -0.0554 | 43 |
| 2014060400 | 2 | 0.5326 | **0** | 0.5937 | 806 |
| 2014060700 | 3 | 0.0230 | 0.5772 | .0230 | 588 |
| 2014071006 | -- | 0.0571 | 0.7644 | 0.0572 | 28 |
| 2014071706 | 4 | 0.4194 | **0.0001** | 0.4469 | 79 |
| 2014080700 | -- | 0.2313 | **0** | 0.2355 | 477 |
| 2014082706 | -- | 0.2554 | **0.0111** | 0.2612 | 96 |
| 2015040300 | -- | 0.0738 | 0.3012 | 0.0740 | 196 |
| 2015060500 | 5 | 0.1192 | **0.0391** | 0.1198 | 298 |
| 2015061112 | 6 | 0.2210 | **0** | 0.2247 | 383 |
| 2015062500 | 7 | 0.4348 | **0** | 0.4658 | 261 |
| 2015070812 | 8 | 0.5171 | **0** | 0.5724 | 462 |
| 2015071606 | -- | 0.2503 | **0** | 0.2558 | 429 |
| 2015073012 | -- | 0.1808 | **0.0072** | 0.1828 | 218 |

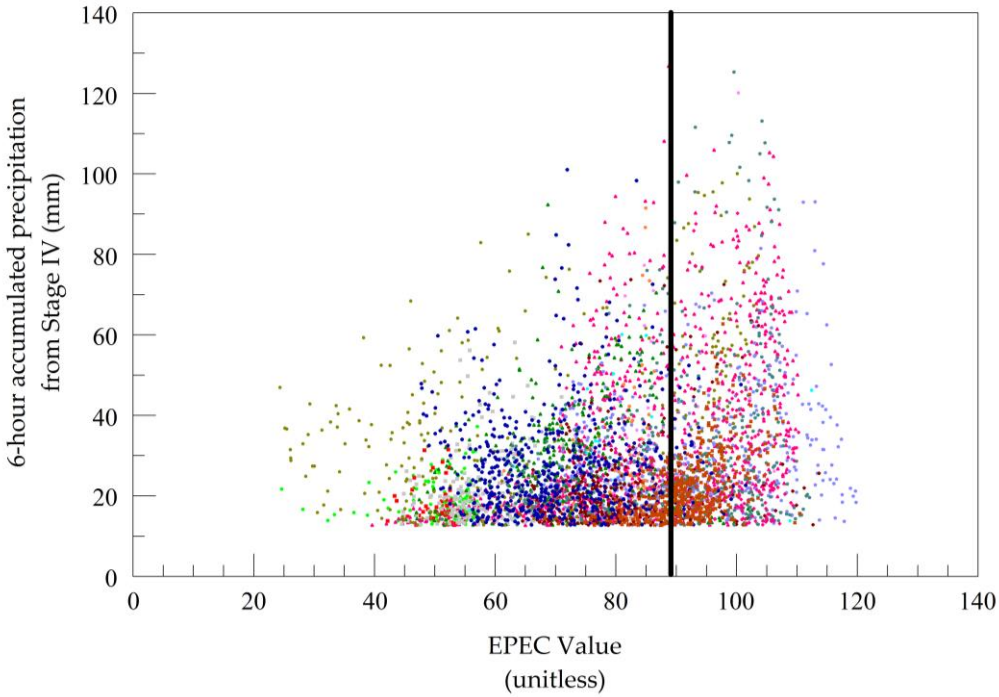


**Figure 4.5. Scatter plot of EPEC values vs. ensuing 6-hour precipitation (mm) for all 15 cases. Threshold value for 6-hour accumulated precipitation is 12.7mm. The bold line is the mean (89) for EPEC.**

Figure 4.5 shows the correlation between the 6-hour accumulated precipitation and EPEC values for all 15 events. There seems to be an upslope trend with the events, where there are events with over 127 mm (5 inches) in 6 hours, with EPEC values greater than the mean (89). Figure 4.5 indicates that there are many events with low precipitation values and low-to-high EPEC values.

All 15 events were analyzed and ran through the FORTRAN code, which produced statistical values for POD, FAR, CSI and the bias for each individual event. Table 4-2 shows the results the 15 events, which include the IOPs where the PRECIP project deployed.

**Table 4-3: Each event and its associated probability of detection (POD), false alarm ratio (FAR), critical success index (CSI), and bias value. Bold values are the significant values for each statistic for associated events.**

| Date | IOP | POD | FAR | CSI | Bias |
|---|---|---|---|---|---|
| 2014040206 | 1 | 0 | NAN | 0 | 0 |
| 2014051018 | -- | 0 | NAN | 0 | 0 |
| 2014060400 | 2 | **0.710** | **0.164** | **0.623** | **0.850** |
| 2014060700 | 3 | 0.361 | **0.255** | **0.321** | 0.485 |
| 2014071006 | -- | **0.767** | 0.772 | 0.213 | 3.367 |
| 2014071706 | 4 | **0.938** | 0.618 | **0.373** | 2.457 |
| 2014080700 | -- | **0.871** | 0.677 | **0.308** | 2.695 |
| 2014082706 | -- | **0.847** | 0.935 | 0.064 | 13.01 |
| 2015040300 | -- | 0.096 | 0.604 | 0.084 | 0.242 |
| 2015060500 | 5 | 0.409 | 0.749 | 0.184 | 1.637 |
| 2015061112 | 6 | **0.748** | 0.744 | 0.235 | 2.932 |
| 2015062500 | 7 | 0.392 | 0.772 | 0.168 | 1.719 |
| 2015070812 | 8 | **0.991** | 0.634 | **0.365** | 2.709 |
| 2015071606 | -- | **0.817** | 0.648 | **0.326** | 2.323 |
| 2015073012 | -- | **0.936** | 0.767 | 0.229 | 4.018 |
| | | | | | |
| 15 Cases | | 9 > 0.5 | 2 < 0.5 | 6 > 0.25 | |

There were a total of 9 events that had a probability of detection (POD) value greater than 0.5. Based on Jolliffe & Stephenson (2003) a POD value close to 1 is considered to be a perfect score. This suggests that these 9 events were more correctly forecasted to some degree (shown bold in table 4-3). POD is highly sensitive to missed events rather than false alarms. EPEC did not accurately predict a portion of the events, those with a POD value with less that 0.5. There are two events where the POD score is zero, implying that EPEC did not forecast the heavy rainfall that occurred. These two events more than likely had EPEC values less than the 25$^{th}$ percentile, which was the minimum threshold set in the FORTRAN code.

There were two events with a FAR value less than 0.5, which needs to be near 0 to be considered a decent score (shown bold in Table 4-3). These scores show the fraction of events that actually occurred. Two events did not have a FAR score because the event was not correctly forecasted and/or had EPEC values less than the $25^{th}$ percentile. The other 11 events had a FAR score greater than 0.5, which implies that there are more false alarms with these events. This is due to FAR being more sensitive to false alarms while ignoring missed events. An example of a false alarm, a hit, and a miss is shown in Figure 4.5.

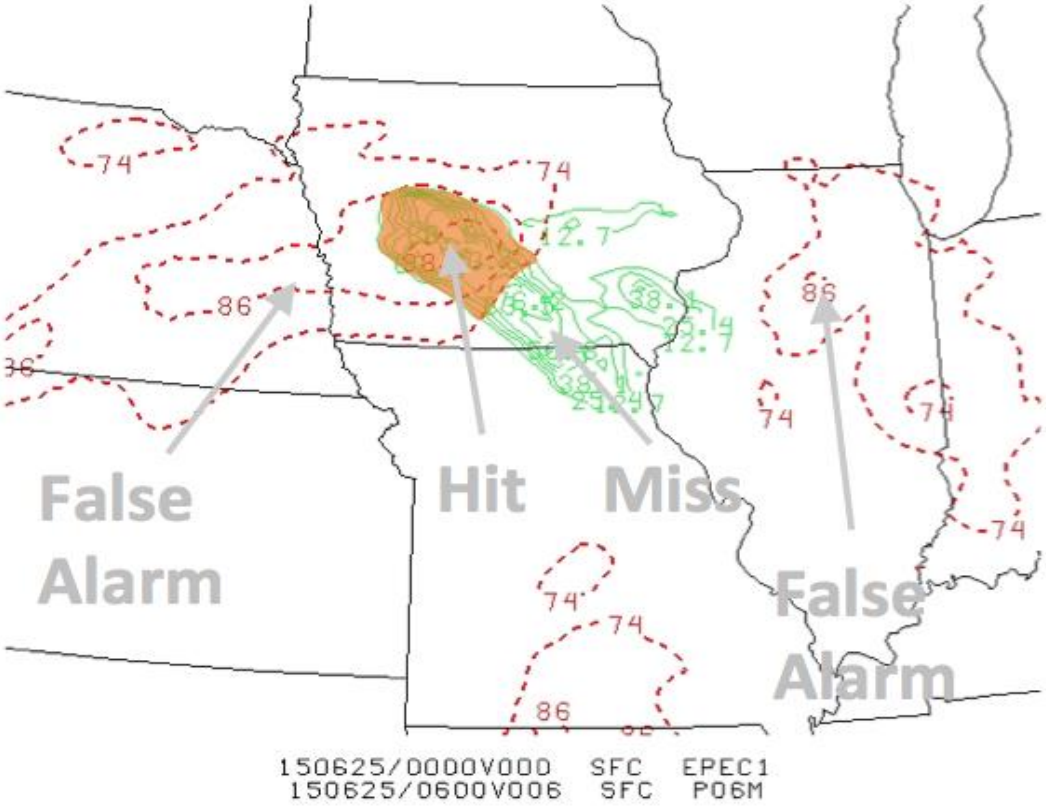


**Figure 4.6: Image showing what a false alarm, a miss, and a hit represents.**

There were 6 events with a CSI value greater than 0.25, which is statistically significant for these data (shown bold in Table 4-3). This suggests that these events had more than ¼ of the event correctly predicted while the other events are closer to zero and were less predicted than the others. The bias numbers closer to 1 means that there is less bias, while the numbers father away from 1 suggest the event was over-biased and the numbers closer to zero implies an under-biased event. The results of the bias show that 3 out of 15 events were not over-forecasted, while 10 of the 15 were over-forecasted.

The statistical analysis between the EPEC index and the Stage IV precipitation data for all 15 events show that there is a positive linear relationship between the two values. There were 9 events with significant probability of detection, while only 2 events

had a false alarm ratio close to zero. This indicated that there are many false alarms produced when EPEC is used for forecasting heavy rainfall with elevated convection. This can also be seen based on the high bias numbers that show EPEC over-forecasting the most of the events.

Clearly, the EPEC index overforecasts areas of heavy precipitation with elevated convection, when used on its own. Yet, the EPEC index is meant to assist with identifying regions of heavy rainfall associated with elevated convection. Despite EPEC over-forecasting events, the index can still point forecasters in right direction to where there could be a possibility of heavy rainfall. Guidelines for EPEC use are shared in Chapter 5.

## 4.3 Comparison of EPEC to Climatology

In addition to the basic statistical evaluation just presented, the typical EPEC values are now compared to calculated climatological values of EPEC. Using mean K Index values for the Plains States (DeRubertis 2006), climatological precipitable water values for Topeka, Kansas (Storm Prediction Center 2016), and an assumed mean divergence at 250 mb of 0, average EPEC values can be estimated. Additionally, using the first standard deviation above the mean for 1) K Index values for the Plains States (DeRubertis, 2006), and 2) precipitable water values for Topeka, Kansas (Storm Prediction Center, 2016), and assuming a positive divergence value at 250 mb of $5 \times 10^{-5}$ $s^{-1}$, the first standard deviation above mean EPEC values can be estimated.

Table 4-4 shows the mean climatological values of the components, and how they sum to EPEC values of 31.4 (60.7) for the spring (summer) seasons. These values fall

**Table 4-4. Mean values of precipitable water (PW; mm), K-index (KINX; unitless), and 250-hPa divergence (x10$^{-5}$ s$^{-1}$; DIV), and EPEC (unitless). These mean values are for the spring and summer seasons.**

| | PW | KINX | DIV | EPEC |
|---|---|---|---|---|
| Spring | 17.0 | 14.4 | 0 | 31.4 |
| Summer | 32.8 | 27.6 | 0 | 60.7 |

**Table 4-5. Values for the first standard deviation above the mean of precipitable water (PW; mm), K-index (KINX; unitless), and 250-hPa divergence (x10$^{-5}$ s$^{-1}$; DIV), and EPEC (unitless). These mean values are for the spring and summer seasons**

| | PW (1.5 S.D.) | KINX (1.5 SD) | DIV | EPEC |
|---|---|---|---|---|
| Spring | 25.1 | 15.9 | 5 | 46 |
| Summer | 41.7 | 29.1 | 5 | 75.8 |

below the mean EPEC value (89) in the same setting, as well as the first standard deviation below the mean for EPEC value (81.5) in elevated heavy rain situations. Table 4-5 also features EPEC values calculated using the first standard deviation above the mean. These values are larger, with 46 (75.8) for the spring (summer) season. Even so, the best of them is still below the 25th percentile for EPEC value (81.5) in elevated heavy rain situations. This suggests that EPEC performs well in identifying heavy rain events in atmospheres that exceed climatology.

## 4.4. Best and Worst Case

In order to answer the question of how does EPEC indicate heavy rainfall; two cases are thoroughly analyzed. This analysis was conducted to present the best and worse case for the EPEC parameter and to determine why they did (not) work. The analysis will cover what was previously forecasted by the PRECIP project, how the events were ranked, synoptic analysis, and a review of the statistical results.

### 4.4.1. 04 June 2014

The best case occurred on June 04, 2014, which is also known as IOP-2. This event when forecasted by the PRECIP project 48 hours prior to the start of the heavy rainfall event. The event was showing signatures from prior composite studies (McCoy, 2014). The target area for heavy rainfall was to occur over the southern half of Iowa during the early morning hours. Based on McCoy's (2014) composites the target area was narrowed down to southwest Iowa. Going forward 24 hours, PRECIP's target area shifted slightly north. The heavy rainfall was to occur due to a warm front moving northeast from northern Missouri. Precipitable water values were in excess of 38.1 mm (1.50 inches) in parts of Missouri. During this time the National Weather Service had issued flash flood watches for southern Iowa and northern Missouri. Soundings were also indicating significant elevated instability from KDSM (Des Moines, IA). Figure 4.6 shows where the PRECIP project had forecasted for heavy rainfall and where the two vans were to setup to conduct balloon launches. A northern van would deploy to Stuart, IA, while a southern van would be in Bethany, MO. The teams were placed just to the north and south of where the heaviest rainfall was forecasted to be for Day 1 (June 04, 2015).

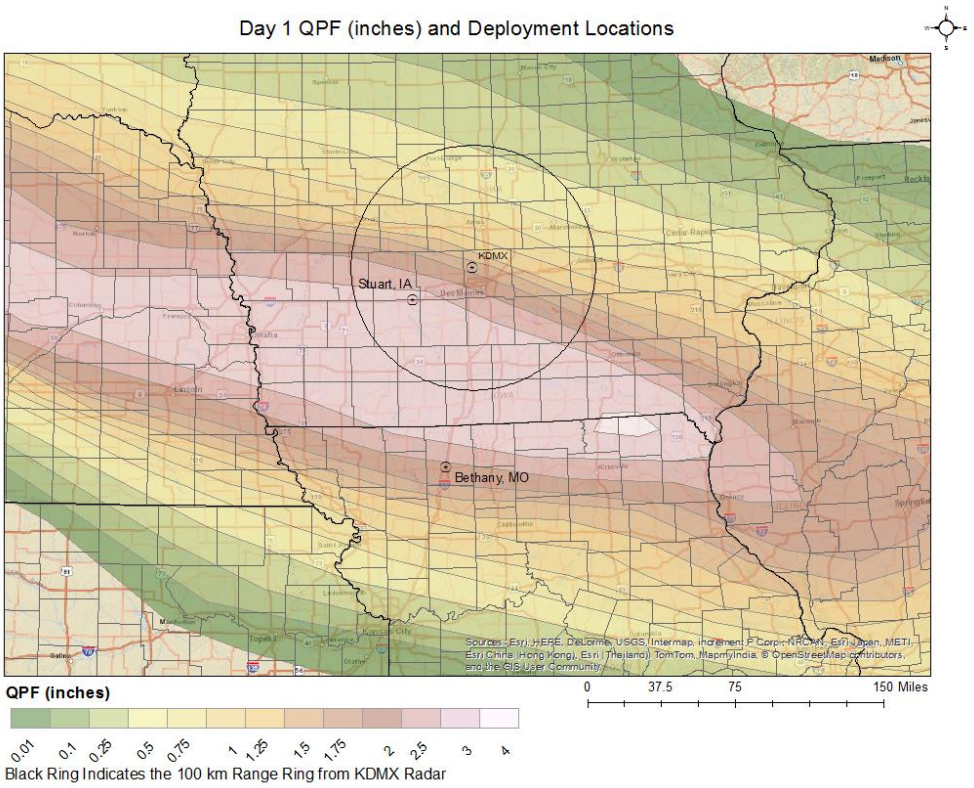


**Figure 4.7. Map of rainfall (inches) predicted to occur and the locations of the PRECIP teams deployment vans.**

Looking at Figure 4.7 the most significant precipitation occurred to south of where the PRECIP project had forecasted, which was between the two sounding locations where the PRECIP teams were deployed. A significant MCS developed over the cold air just to the north of a warm frontal boundary. Based on the surface analysis (Figure 4.8) from the Weather Prediction Center the rainfall that occurred in Iowa and part of northern Missouri was to the north of the warm front, which is in the cold sector and indicates that this was an elevated event associated with heavy rainfall.

This event was prior to when EPEC was created and the index was therefore not used in PRECIP's early forecasts in 2014. Despite this setback EPEC was able to be reproduced and plotted for this event. EPEC contours 24 hours prior to this event

highlighted heavy precipitation shown in Figure 4.7 with values greater than 74 ($25^{th}$ percentile). The red dashed lines indicate EPEC values greater than the $25^{th}$ percentile (74), while the green solid lines represents the 6-hour precipitation in millimeters with values greater than 12.7 mm (1.50 inches). EPEC highlights the majority of the heavy rainfall, while there is only one false alarm. Figure 4.7 shows that EPEC did miss part of the rainfall in central Missouri.

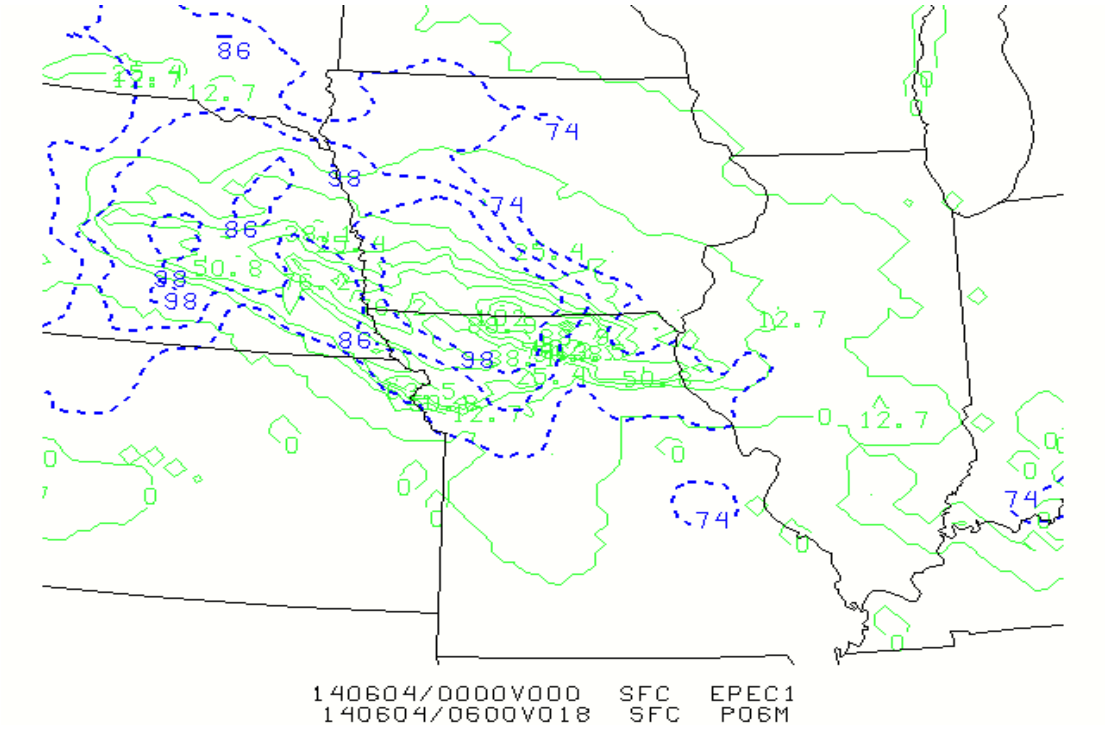


**Figure 4.8. 6-hour accumulated precipitation (solid green, every 12.7mm) ending at 0600 UTC while EPEC values are in dashed blue at 0000 UTC (contoured in 25th, 50th, and 75th percentiles).**

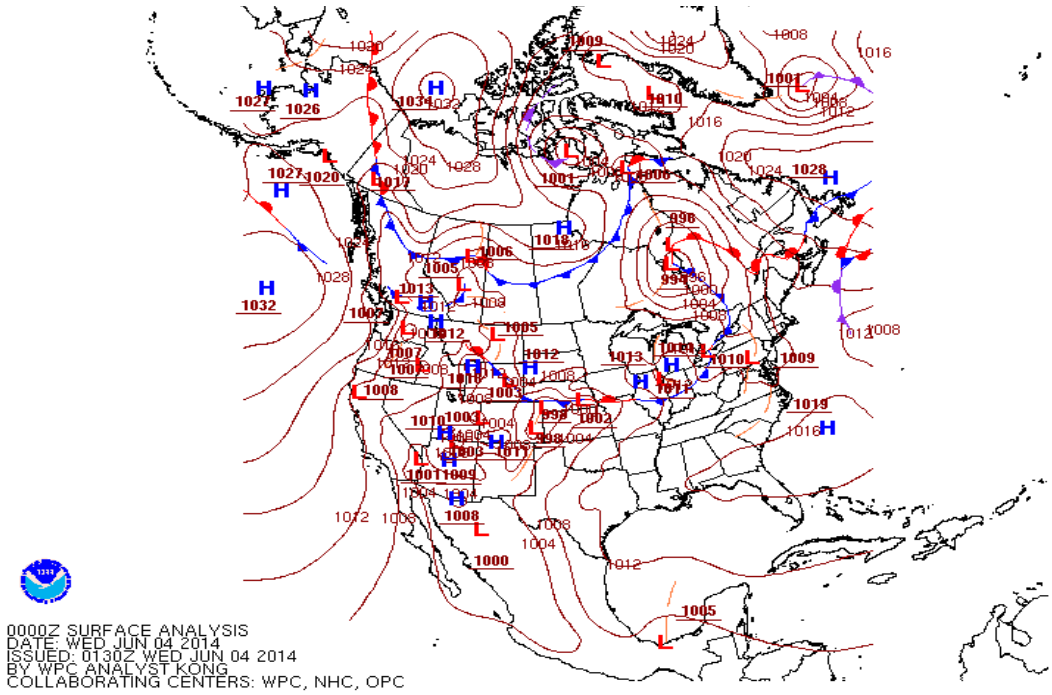


**Figure 4.9. Surface analysis at 0000 UTC on 04 June 2014 from the Weather Prediction Center.**

When the subjective rankings were completed IOP 2 was ranked as a 1 using the GFS211 and a 2 using the NAM 211, which is based on where EPEC predicted where the heavy rainfall happened 36 hours prior to the actual occurrence. Figure 4.9 shows storm total precipitation at the time of the maximum rainfall occurrence with the 36-hour forecasted EPEC index using the GFS 211, while Figure 4.10 shows the same event using the NAM 211. The GFS 211 displaced maximum values of EPEC off to the east in northern Illinois of the actual event, while the NAM 211 shifted the maximum slightly to the northeast of the event. EPEC still did not highlight the entirety of this event 36 hours prior to the event. However, when EPEC was plotted 6 hours prior to the actual occurrence of the heavy rainfall event (figure 4.7), EPEC did highlight the entirety of the rainfall. The results underscore 1) the utility of the EPEC value, and 2) that EPEC is prone to error to the extent that parent model solutions are prone to error, like any other parameter, derived (CAPE) or empirical (K-index).

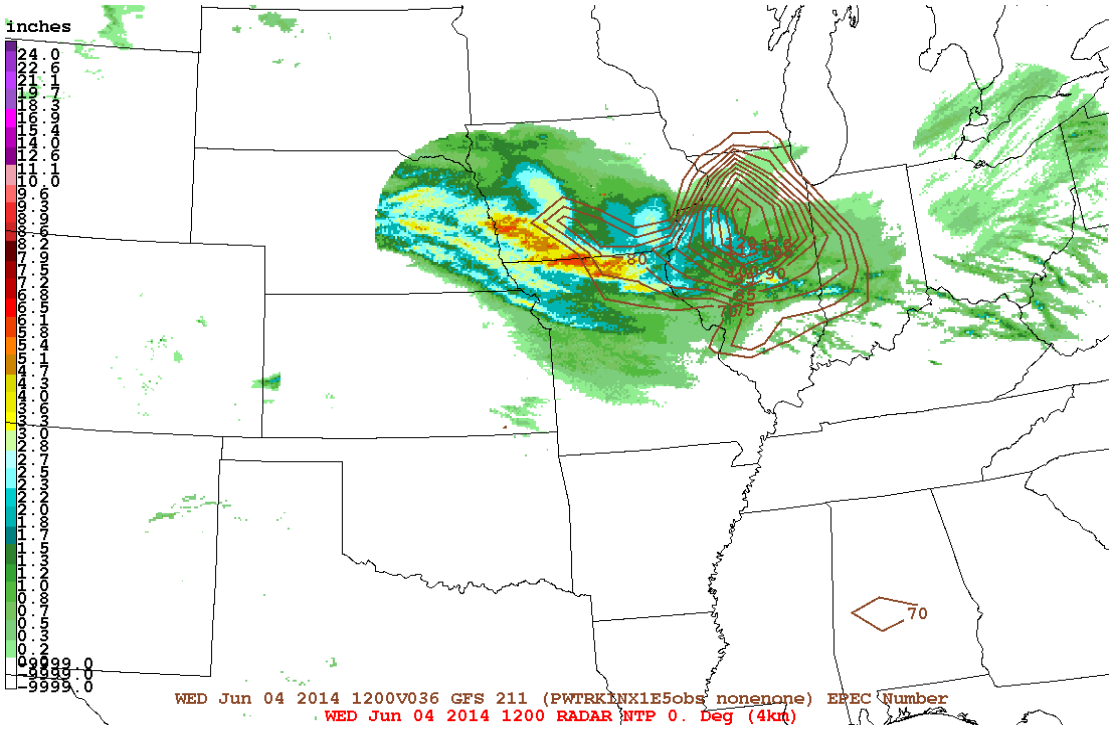


**Figure 4.10. Storm total precipitation at the time of the maximum rainfall occurrence with the 36-hour forecasted EPEC index using the GFS 211; format as in Fig. 4.1.**

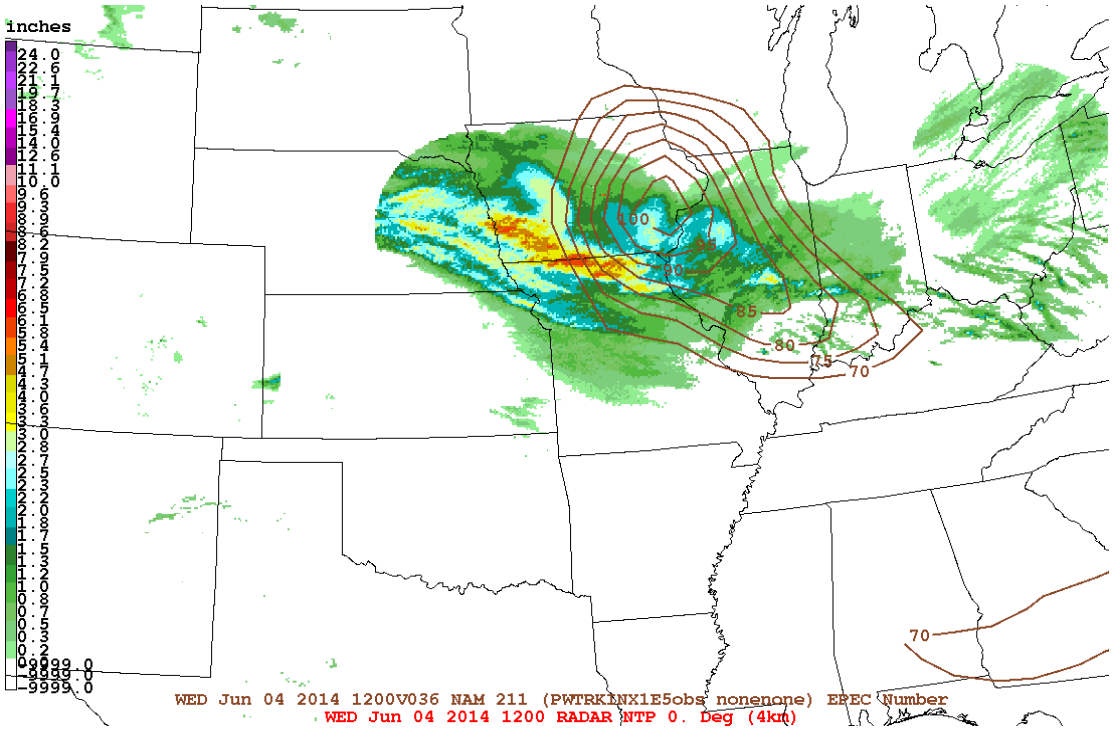


**Figure 4.11. Storm total precipitation at the time of the maximum rainfall occurrence with the 36-hour forecasted EPEC index using the NAM211; format as in Fig. 4.1.**

The 250-hPa analysis for 04 June 2014 (IOP 2) was analyzed at 0000 UTC, which is the same time that EPEC was plotted with 6-hour precipitation (Figure 4.11). There is a small trough located in the northwest part of the CONUS while a secondary trough has also formed off the west coast. The heavy rainfall event occurred in the right entrance region of the jet streak that is located in across Michigan, Wisconsin, and parts of Minnesota and Iowa. According to Lackmann (2011), this area lies within the right entrance region of an upper-level jet streak is associated with ascent and forcing that is provided by a cyclonic vorticity advection that increases with height. Plotting divergence with the height field shows that there is a large area of divergence where the heavy rainfall event occurred in Iowa. Ninomiya (1971) suggested that strong divergence near the upper-troposphere in the close-to-the-storm region can be recognized by the significant upward transport of mass and latent heat release during condensation.

At 500 hPa, the same two troughs at 250 hPa can be seen still in the northeast and the west coast of the CONUS (Figure 4.12). A few shortwaves can be seen in the height pattern in northern Missouri, which initiated an area of circulation in southern Iowa and northern Missouri. These shortwaves can be attributed to areas of instability in the atmosphere.

The surface analysis at 0000 UTC 04 June 2014 shows that a low pressure system is located in eastern Colorado. This low pressure will be bringing in moisture in from the Gulf into the area of the event. Plotting $\Theta_e$ over the mean sea-level pressure will help identify where there are frontal boundaries and where the cold sector is located, which helps verify if the rainfall that occurred was associated with elevated convection. Looking at 950-hPa $\Theta_{e,}$ there is a weak boundary that extends from central Nebraska into

the southwest corner of Iowa (Figure 4.13). By looking at $\Theta_e$ it can be seen that the heavy rainfall event did occur on the cold side of the boundary, which is where the lower $\Theta_e$ values are located.

Figure 4.14 shows K-index values and precipitable water (inches) values at 0000 UTC on 04 June 2014. K-index values range from 25 to 40 near the region of where the heavy precipitation occurred. K-index values greater than 30 are considered to have a strong signal and small variability when associated heavy rainfall producing elevated thunderstorms (McCoy, 2014). Also precipitable water values were between 38.1 to 44.5 mm (1.50 to1.75 inches) near the event. This event did have flash flood watches issued by the National Weather Service in southern Iowa and northern Missouri.

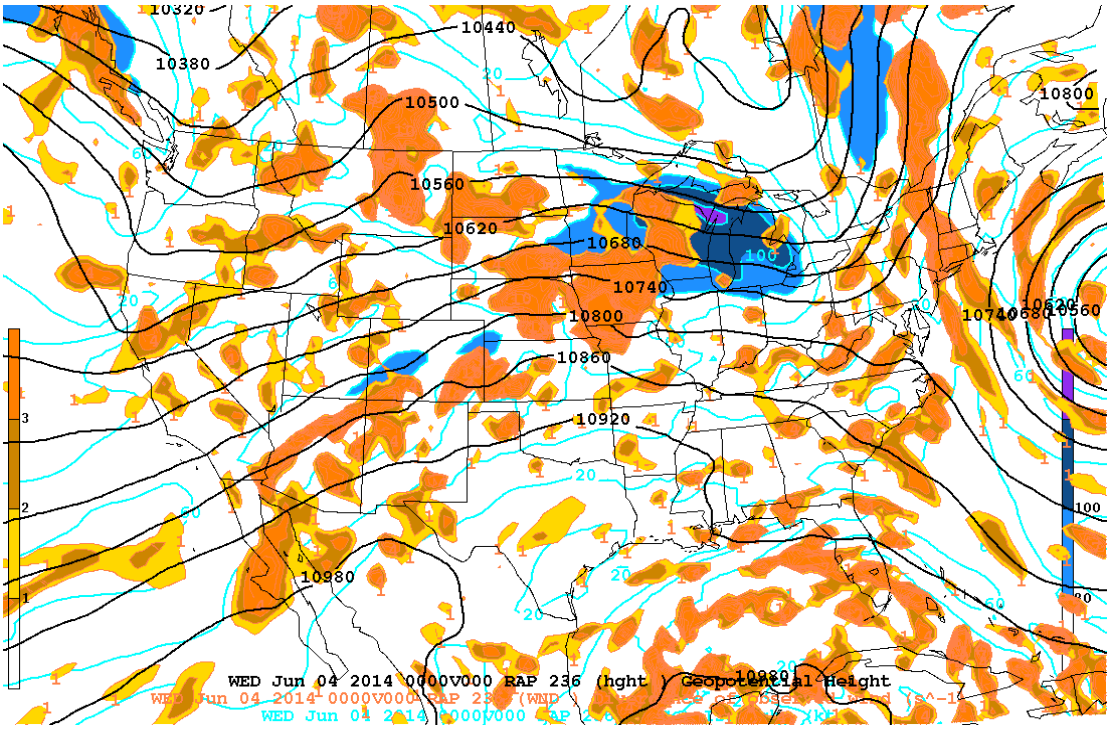


**Figure 4.12. 250-hPa geopotential heights (every 120 gpm, solid black), 250-hPa winds in knots (every 20 knots, solid blue, shaded above 80 knots), and 250-hPa divergence (shaded every 1 $s^{-1}$) at 0000 UTC on 04 June 2014.**

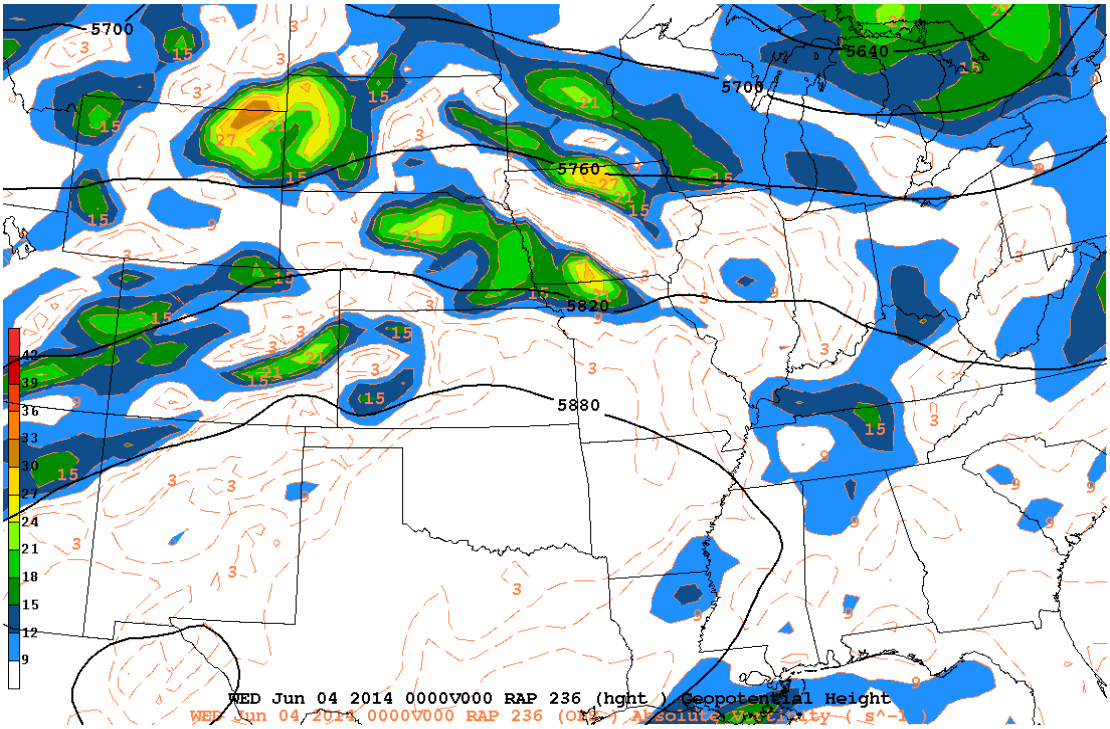


**Figure 4.13. 500-hPa geopotential heights (every 60 gpm; solid black) and 500-hPa absolute vorticity (dashed brown interval 3 $10^{-5}$ $s^{-1}$, shaded above 9 X $10^{-5}$ $s^{-1}$) at 0000 UTC 04 June 2014.**

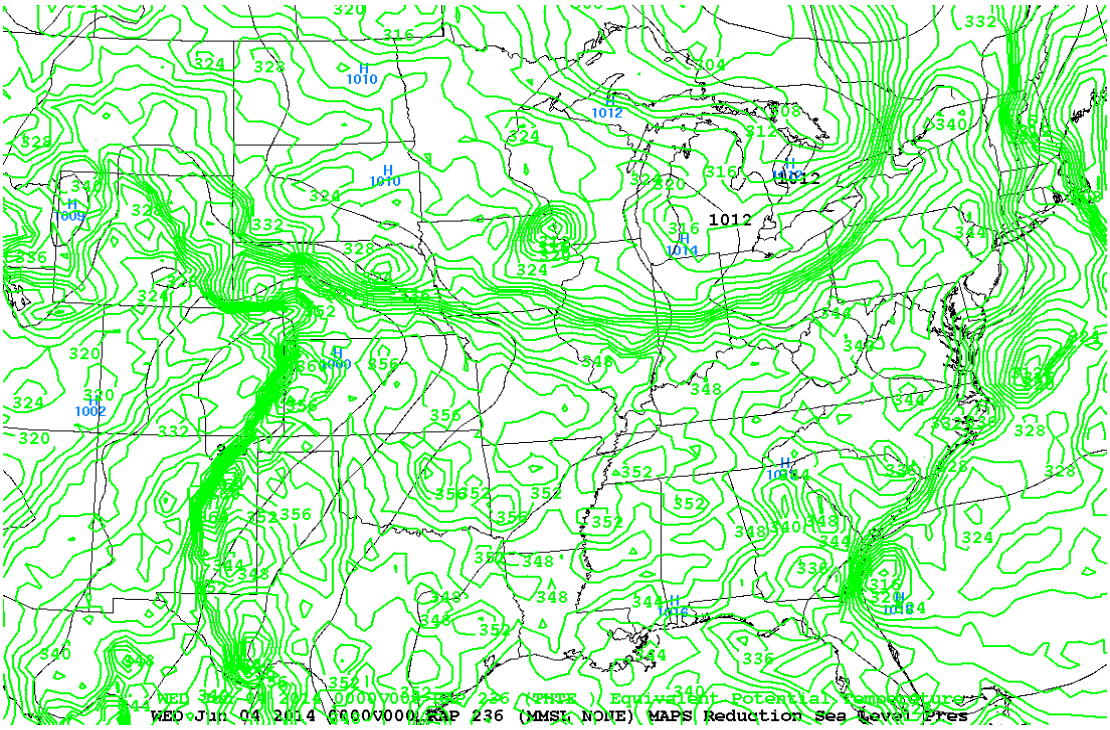


**Figure 4.14: Mean sea level pressure (solid black; every 4 hPa) and 950-hPa $\Theta_e$ (solid green; every 2K) 0000 UTC 04 June 2014.**

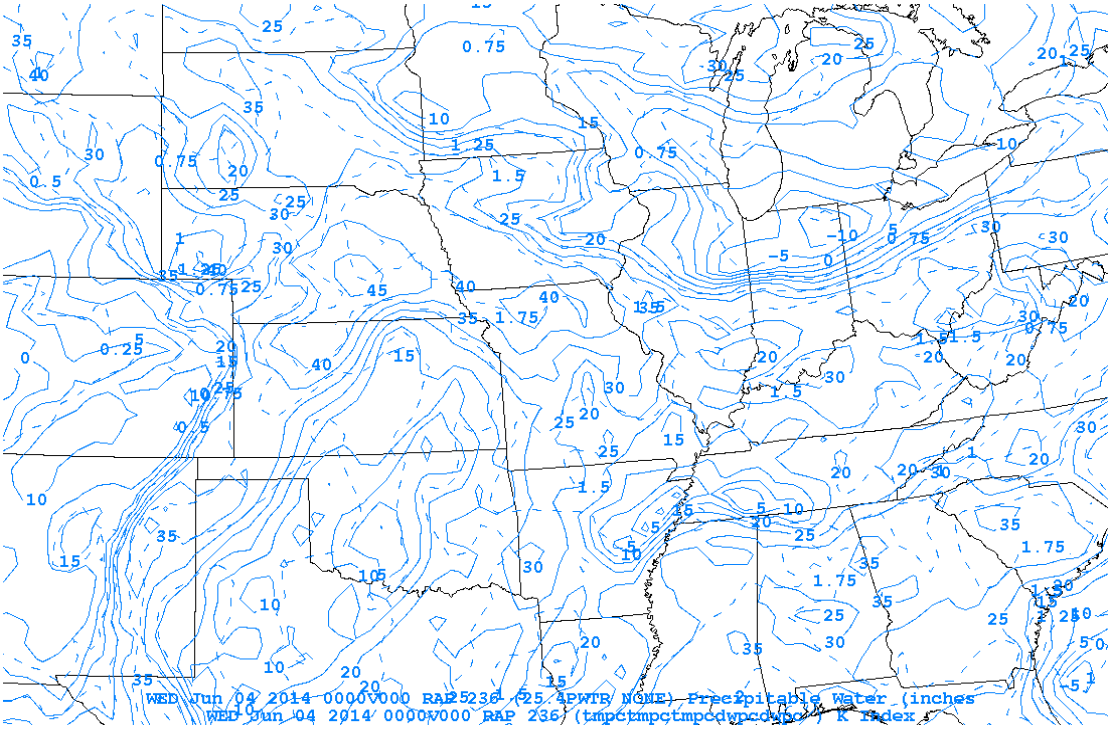


**Figure 4.15: Precipitable water in inches (solid blue, interval 0.25 inches) and K-index (dashed blue, every 5) at 0000 UTC on 04 June 2014.**

Taking a look back at Table 4-1 shows the correlation coefficient for 04 June 2014 has a value of 0.656, while the probability matrix has a value of zero. These values indicate that there is a strong linear relationship between the 6-hour precipitation and the forecasted EPEC. This event also had 220 degrees of freedom, which is the highest out of all the events. IOP 2 was also the case where POD, FAR, CSI and bias showed statistical significance (Table 4-2). With values of POD being 0.764 and FAR being 0.138, which indicates that EPEC was able to correctly forecast the majority of observed heavy precipitation.

The event on 04 June 2014 was considered to be one of the best cases for the EPEC parameter. The subjective analysis showed that this event was ranked as a 1 for the GFS 211 and a 2 for the NAM 211. Despite this low ranking, the statistical results indicated the opposite. Values of high probability of detection, low false alarm ratio, and an extremely positive correlation coefficient were calculated for this event. These statistical results indicate significant values for this elevated thunderstorm case.

### 4.4.2. 10-11 May 2014

An event that occurred on 11 May 2014 was initially forecasted by the PRECIP team 48 hours prior to the actual occurrence. McCoy's composites were suggesting an event to occur in parts of Kansas. A divergence maximum was positioned over a location of maximum convergence in southeastern Kansas. As the jet streak increased across northeastern Kansas so did the divergence maximum near northwestern Missouri. There was plenty of moisture present with precipitable water values exceeding

1.50 inches. The PRECIP team expected significant elevated convection, but the event was a little too far north of the study area at the time.

The 24-hour forecast for this event did not change dramatically but the location did change. The GFS and NAM forecasted for a warm front to move through Missouri and eastern Kansas on 10 May and the front would be slowing down around 0000 UTC in northern Missouri and southern Iowa. The best moisture pooling was located in northwestern Missouri. K-index exceeded the composite threshold (McCoy, 2014), while precipitable water values were above normal by ~ 125%. The PRECIP team was anticipating elevated convection, but precipitation was likely to form south of the warm front and they were not expecting heavy rainfall across the study area. WPC's surface analysis at 1800 UTC (Fig. 4.16) shows a warm front was analyzed in northern Missouri, which is south of where the precipitation actually occurred. Comparing Figure 4.15 and Figure 4.16 shows that the rainfall did occur north of the warm front indicating that this event is associated with elevated convection. In Figure 4.15 EPEC is not present for this event, this is possibly due to EPEC being less than the $25^{th}$ percentile (74).

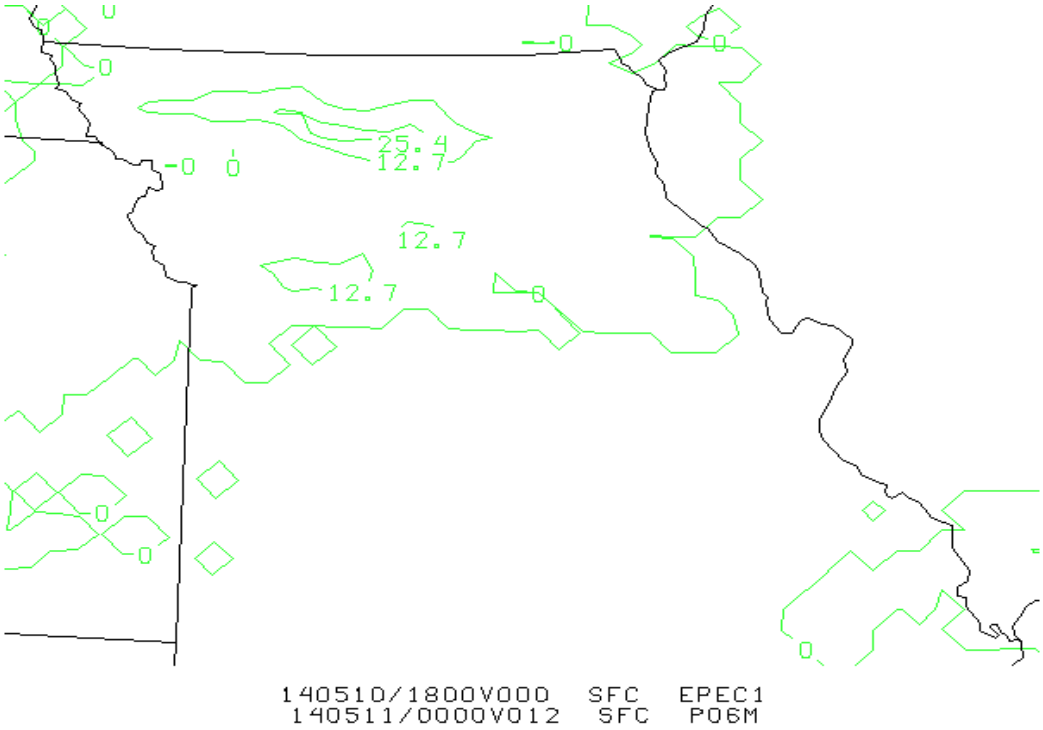


**Figure 4.16. 6-hour accumulated precipitation (solid green, every 12.7mm) ending at 0000 UTC while EPEC values are in dashed blue at 1800 UTC (contoured in 25th, 50th, and 75th percentiles).**

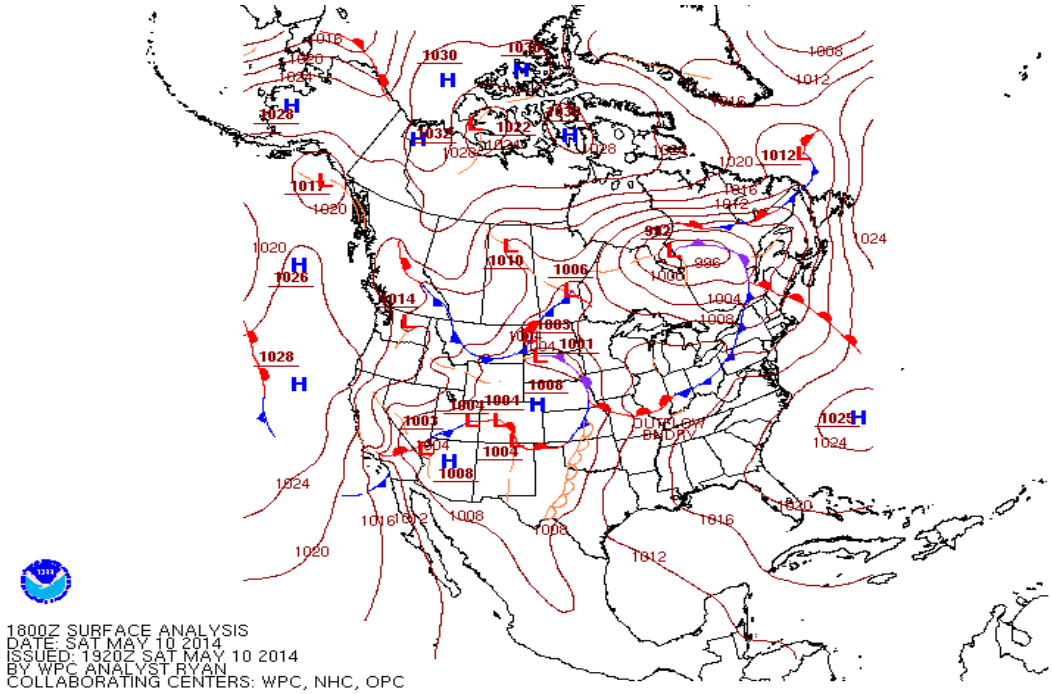


**Figure 4.17. Surface analysis at 1800 UTC on 10 May 2014 from the Weather Prediction Center.**

The event on 10-11 May 2014 was ranked as a 1 for the NAM and a 0 for the GFS (Table 4-2), due to EPEC being displaced. Figure 4.17 shows the NAM 211 forecast for EPEC, which was slightly displaced to the southwest of the event, while the maximum EPEC value was greater than the 25$^{th}$ percentile. Figure 18 shows the GFS 211 forecast for EPEC, which only highlighted a small area to the east of the event.

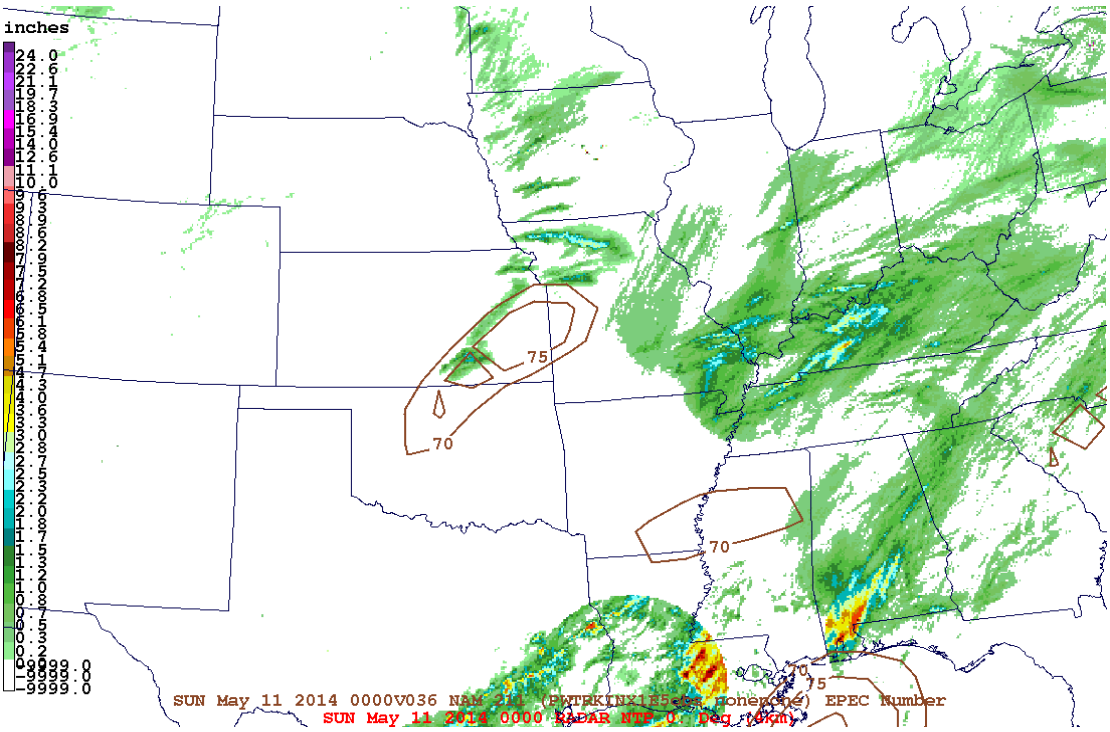


**Figure 4.18. Storm total precipitation at the time of the maximum rainfall occurrence with the 36-hour forecasted EPEC index using the GFS 211; format as in Fig. 4.1.**

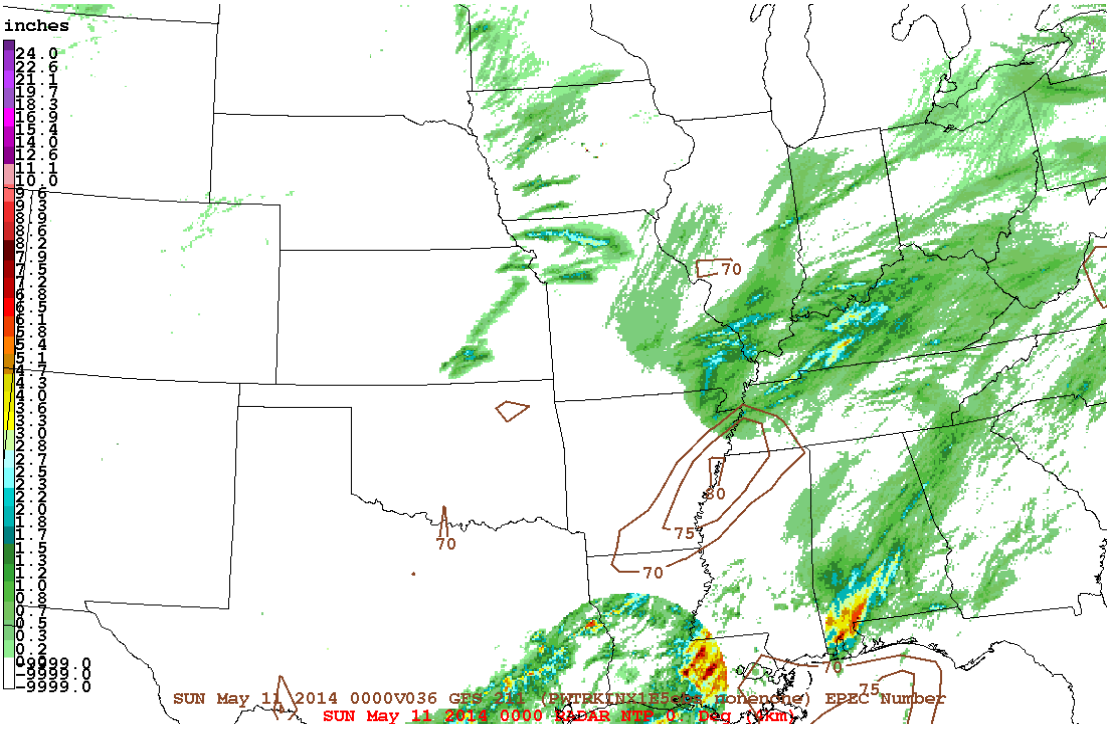


**Figure 4.19. Storm total precipitation at the time of the maximum rainfall occurrence with the 36-hour forecasted EPEC index using the GFS 211; format as in Fig. 4.1.**

The 250-hPa analysis (Fig. 19) for 10 May 2014 at 1800 UTC shows a short ridge to the east of Missouri. The polar upper-level jet streak, around 80 knots, resides over the middle CONUS, with a maximum of 100 knots in northeastern Missouri. There is a small area of divergence in northern Missouri and parts of Missouri.

The 500-hPa heights and vorticity analysis (Fig.4.20) show a series of shortwaves across the CONUS, in which a few areas of circulation have formed. An area of circulation is near the region of heavy rainfall event that occurred in northern Missouri. These areas of circulation will help aid in instability and lift.

A weak low pressure is located in South Dakota at 1800 UTC on 10 May 2014. The boundary across mid-Missouri extends into southeastern Kansas (Fig. 4.21). This boundary was analyzed as a warm front by the WPC (Fig. 4.16). The precipitation that occurred was north of this boundary where the colder $\Theta_e$ values reside.

Figure 4.22 shows K-index and precipitable water analyzed at 1800 UTC on 10 May 2014. K-index values in northern Missouri were between 25 and 30, while precipitable water values were greater 25.4 mm (1 inch). McCoy's composites suggest that these values are significant for heavy rainfall events (McCoy, 2014).

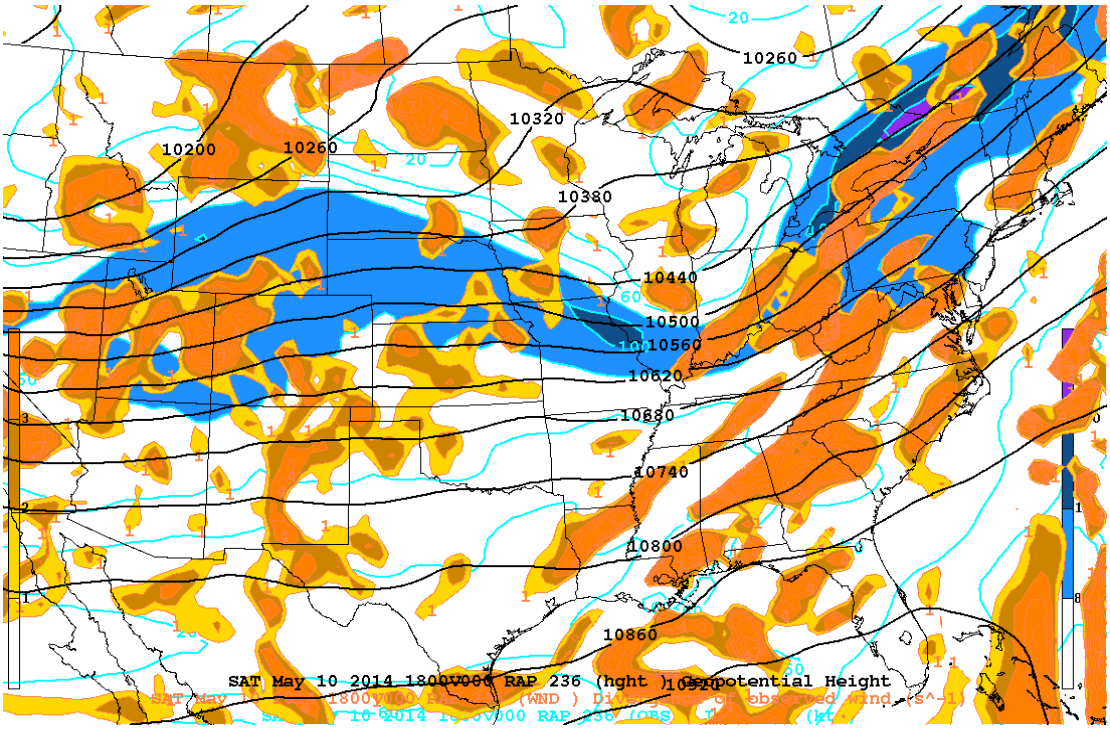


**Figure 4.20. 250-hPa geopotential heights (every 120 gpm, solid black), 250-hPa winds in knots (every 20 knots, solid blue, shaded above 80 knots), and 250-hPa divergence (shaded every 1 $s^{-1}$) at 1800 UTC on 10 May 2015.**

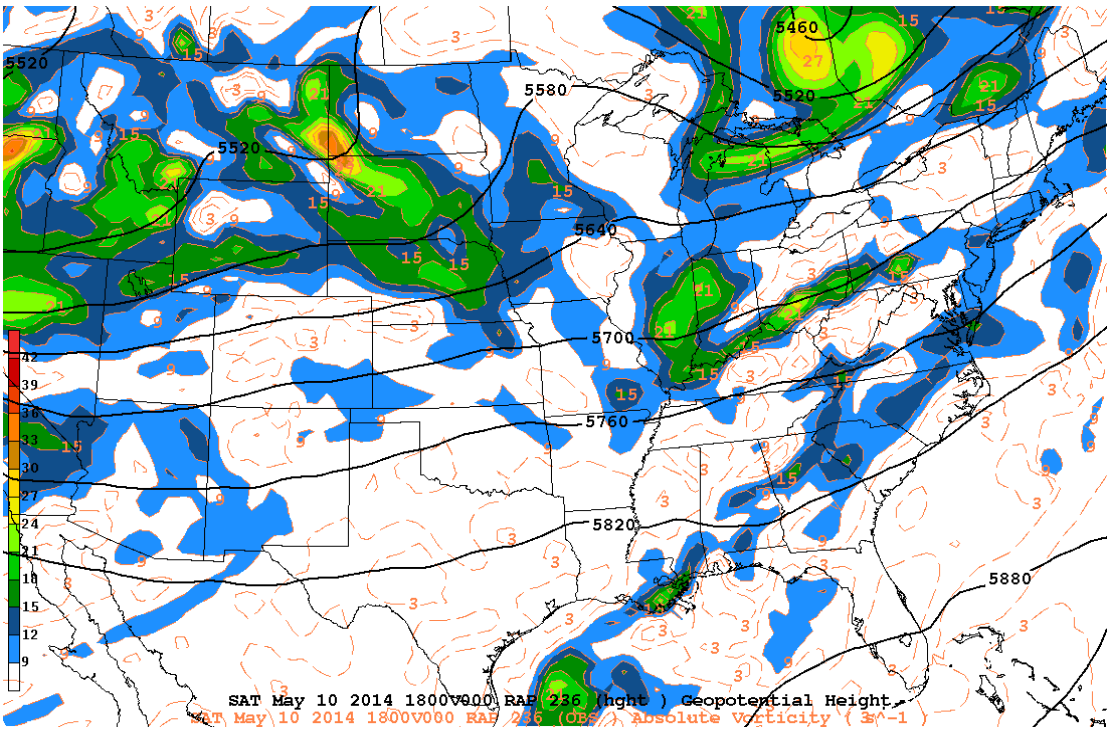


**Figure 4.21. 500-hPa geopotential heights (every 60 gpm; solid black) and 500-hPa absolute vorticity (dashed brown interval 3 X $10^{-5}$ $s^{-1}$, shaded above 9 X $10^{-5}$ $s^{-1}$) at 1800 UTC on 10 May 2014.**

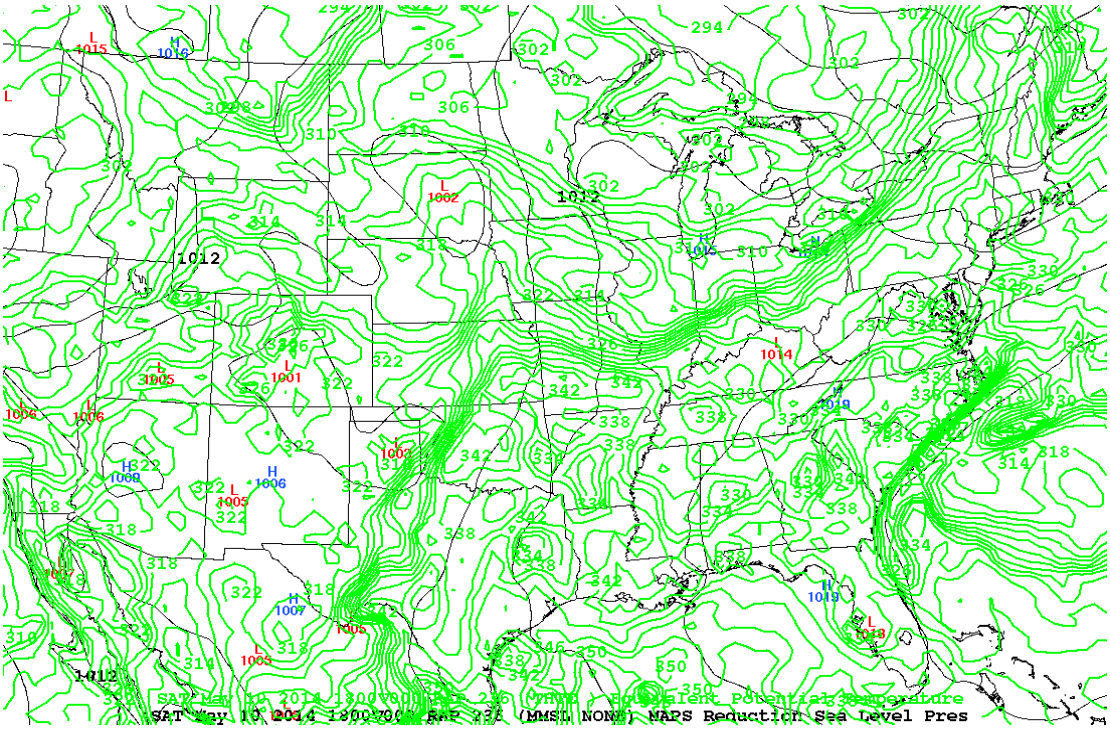


**Figure 4.22. Mean sea level pressure (solid black; every 4 hPa) and 950-hPa $\Theta_e$ (solid green; every 2K) at 1800 UTC on 10 May 2014.**

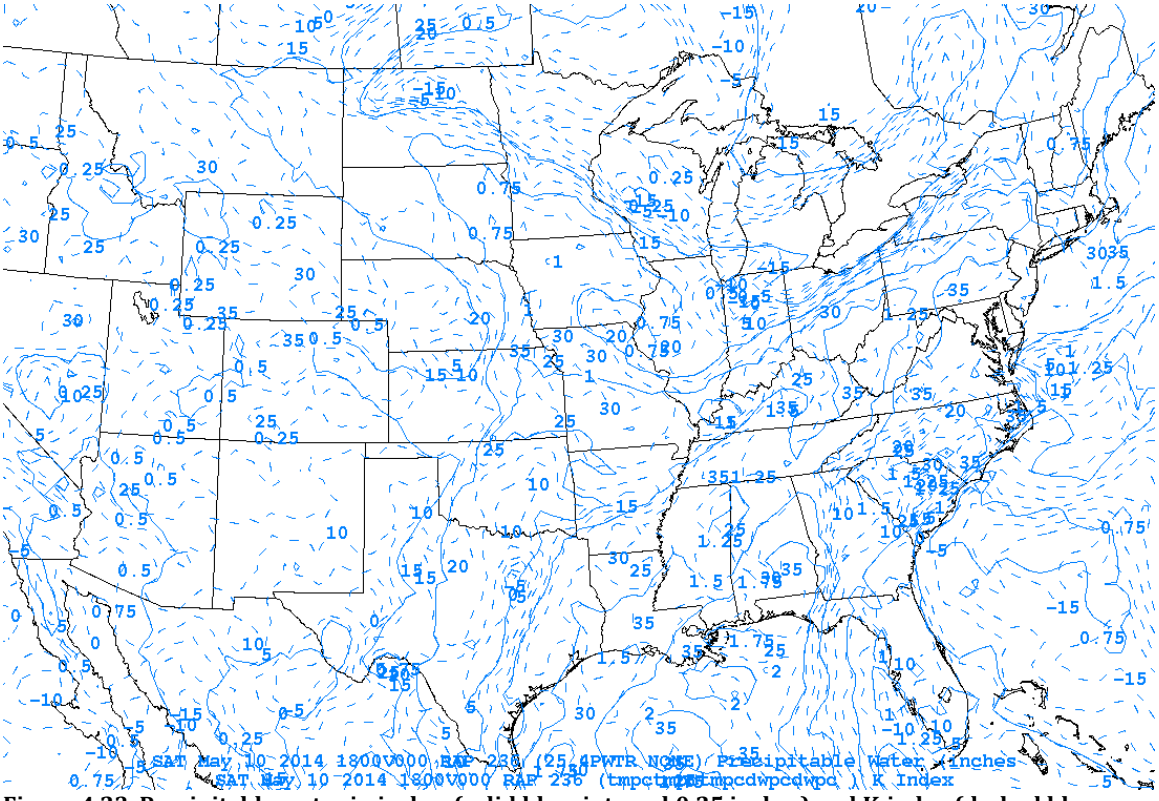


**Figure 4.23. Precipitable water in inches (solid blue, interval 0.25 inches) and K-index (dashed blue, every 5) at 1800 UTC on 10 May 2014.**

This event had a correlation coefficient value that was negative, which was 0.0554 (Table 4-2). This value suggests that there is a slight negative linear relationship to the observed 6-hour precipitation and EPEC. The probability of detection for this event was 0 along with the other CSI and bias (Table 4-3). The reason for this was due to EPEC not correctly forecasting this event (Fig. 4.15).

# Chapter 5. Conclusions

The main objective of this study was to verify if EPEC is a useful predictive parameter for forecasting for flash flooding. This verification was done subjectively by ranking 15 heavy rainfall events and then calculating statistics on the EPEC metric.

Once the events were verified to be associated with elevated convection by comparing the surface analysis field with the actual rainfall occurrence, the 15 events were ranked. The events were ranked on how EPEC forecasted the storm-total precipitation 36-hours prior to maximum rainfall. The results showed that the majority of the events were ranked as a 2 or 3 (on a scale of 0-3) as were the deployments that the Program for Research on Elevated Convection with Intense Precipitation project conducted sounding operations. The PRECIP team generally forecasted extremely heavy rainfall for many of the events. The events that occurred from May through July did have flash flooding associated with them for which the National Weather Service did issued flash flood watches and/or warnings.

Statistical analysis showed that all but 1 of the 15 events had a positive linear relationship between the EPEC index and the 6-hour Stage IV precipitation data. 9 events had a statistically significant probability of detection value greater than 0.5, while only 2 events had a false alarm ratio less than 0.5. We may thus conclude that even though EPEC is able to correctly forecast observed events, the parameter also over-forecasts the events. This is confirmed in the high bias numbers in Table 4-3.

The best (worst) cases for the EPEC parameter were analyzed in order to show how EPEC did (not) work for each event. The best case occurred on 04 June 2014 and was initially ranked low for the NAM 211 and GFS 211 but once statistical analysis was

ran on this event it showed great statistical significance for POD, FAR, and the correlation coefficient. This event did have flash flooding associated with it and Fig. 4.7 shows that EPEC was able to highlight the majority of the heavy rainfall that occurred 6 hours prior to the event with values greater 84, which is the $50^{th}$ percentile. The worst case was quite the opposite in the rankings and statistical analysis. The event on 10-11 May 2014 was initially ranked as a 0 for the NAM 211 and a 1 for the GFS 211 but statistical analysis showed a negative correlation coefficient suggesting a negative linear relationship between EPEC and the 6-hour Stage IV precipitation. There were no statistical values for POD, FAR, CSI due there not being an EPEC value greater than 74. This is can be seen in Fig. 4.15.

As a part of Chapter 4, guidelines were promised regarding the proper employment of the EPEC tool. In keeping with previous work (i.e. McCoy 2014), the focus of EPEC is on the cold side of a thermal boundary. As background, the reliable ingredients for heavy rainfall from elevated convection are highlighted in Fig. 2.3, including:

- A thermal boundary (often a stationary front)
- A jet streak northeast of the heavy rainfall location
- Significant moisture in the deep troposphere to the north of the surface front.

***Additionally*, the EPEC index has shown that there is a positive relationship with heavy precipitation. When EPEC is employed on the cold side of the $\Theta_e$, it can help predict heavy rainfall associated with elevated convection. This parameter is not**

**meant to be used on its own but is meant to aide the forecaster in pinpointing an area of possible heavy rainfall with elevated convection that could lead to flash flooding.**

## 5.1. Future Work

Although our anecdotal experience, and the quantitative results presented here, show utility in the EPEC tool, it can be refined and revised. Possible advances include:

1) Developing a more robust statistical description of the EPEC value (mean and IQR) from the original NARR sounding dataset of McCoy (2014). It is unlikely that the values will change much, but a stronger statistical foundation will emerge.
2) Employing a more equivalent 6-hr precipitation accumulation threshold to McCoy's (2014) 50 mm / 24 hr. Instead of the linear ration used here of 12.7 mm / 6 hr, an exponential ratio 27 mm / 6 hr can be used, which is more befitting the convective precipitation under study here.
3) Replacing the K Index with the most unstable convective available potential energy (MUCAPE) as the instability component of EPEC. While the K Index is more generic and available in most "off the rack" software, it is linked to the precipitable water, and so is not thought of so much as an instability metric.

Of course, other changes could also be made, but these presented above are the ones that seem to have the best potential for a significant and rapid response.

# References


Colman, R. C., 1990: Thunderstorms above frontal surfaces in environments without positive CAPE. Part I: A climatology. *Mon. Wea. Rev*., **118**, 1103-1121.

DeRubertis, D., 2006, Recent trends in four common stability indices derived from U.S. radiosonde observations. *Journal of Climate*, 19, 309-323.

Doswell, C. A., H. E. Brooks, and R. A. Maddox, 1996: Flash flood forecasting: An ingredients-based methodology. *Wea. Forecasting,* **11**, 560–581.

-------, and D. M. Schultz, 2006: On the use of indices and parameters in forecasting severe storms. Electron. J. Severe Storms Meteor.

Grant, B.N., 1995: Elevated cold-sector severe thunderstorms: A preliminary study. *Natl.Wea. Dig*., **19** (4), 25-31.

George, J.J., 1960: *Weather Forecasting for Aeronautics*. Academic Press. p. 673.

Jolliffe, I. T., and D. B. Stephenson, Eds., 2003 *Forecast Verification: A Practitioner's Guide in Atmospheric Science*. John Wiley and Sons, 45-52 pp.

Lackmann, G., 2011: *Midlatitude Synoptic Meteorology: Dynamics, Analysis, and Forecasting.* Amer. Meteo. Soc., 44 pp.

Maddox, R.A., C.F. Chappel, and L.R. Hoxit, 1979: Synoptic and Meso-α Scale Aspects of Flash Flooding. *Bulletin American Meteorological. Society*, **60**, 115-123.

McCoy, L.P., 2014: *Analysis of Heavy-Rain-Producing Elevated Thunderstorms in the MO-KS-OK Region of the United States*.

Moore, J.T., S.M. Rochette, F.H. Glass, and P.S. Market, 1996: Elevated thunderstorms associated with heavy rainfall in the Midwest. Preprints, 18$^{th}$ *Conference on Severe Local Storms*, San Francisco,CA, Amer. Meteor. Soc., 772-776.

Moore, J. T., F. H. Glass, C. E. Graves, S. M. Rochette, and M. J. Singer, 2003: The environment of warm-season elevated thunderstorms associated with heavy rainfall over the central United States. *Weather Forecasting*, **18**, 861-878.

Ninomiya, K., 1971: Mesoscale modification of synoptic situations from thunderstorm development as revealed by ATS III and Aerological Data. *J. Appl. Meteor*., **10**, 1103-1121.

Panofsky, H.A., and G.W. Brier, 1968: *Some Applications of Statistics to Meteorology*. Penn. State University, College of Earth and Mineral Sciences, University Park. 195 pp.

Rochette, S. M., and J. T. Moore, 1996: Initiation of an elevated mesoscale convective system associated with heavy rainfall. *Weather Forecasting*, **11**, 443–457.

Schumacher, R. S., and R. H. Johnson, 2006: Characteristics of U.S. extreme rain events during 1999–2003. *Weather Forecasting*, **21**, 69–85.

*SPC Sounding Climatology Page*. Storm Prediction Center, 24 April 2016. <http://www.spc.noaa.gov/exper/soundingclimo/>.